iScience

CellPress
OPEN ACCESS

Article

A virtuous cycle operated by ERp44 and ERGIC-53 guarantees proteostasis in the early secretory compartment

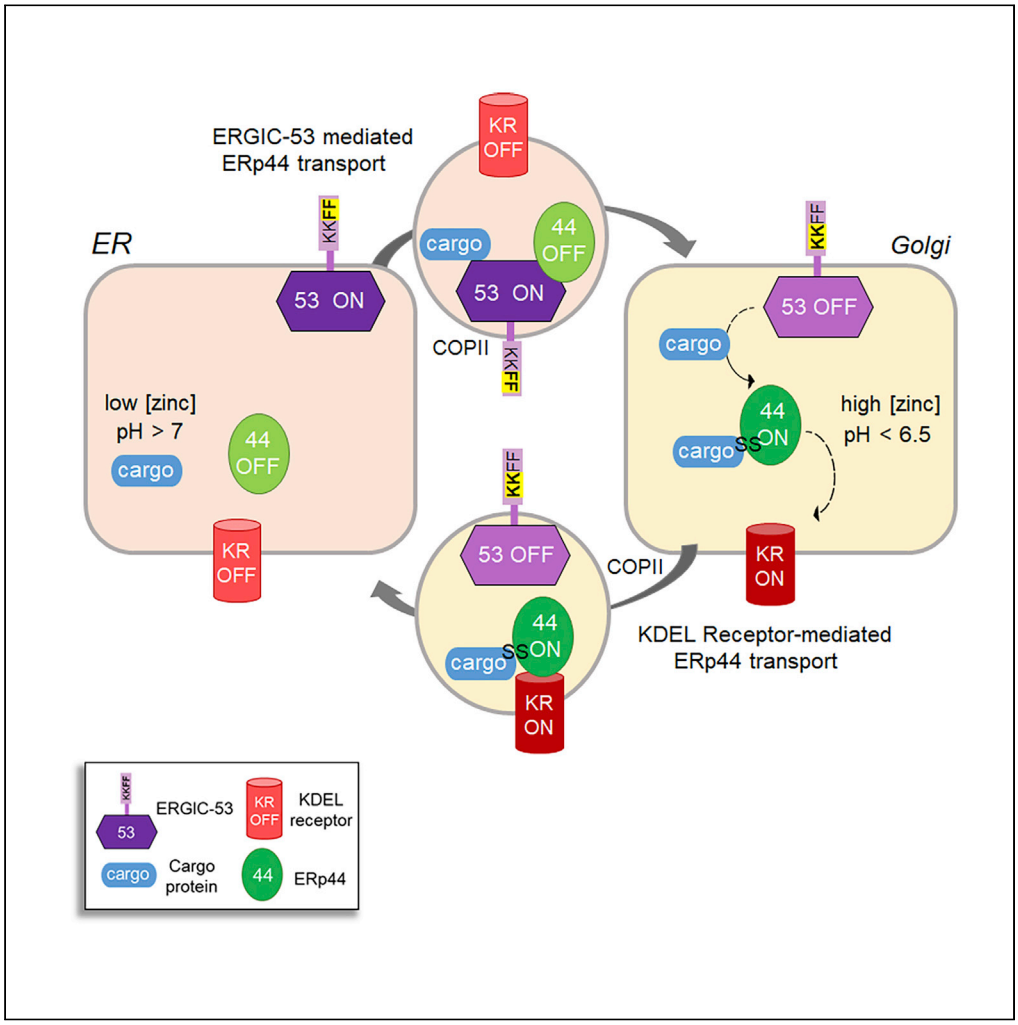

Tiziana Tempio, Andrea Orsi, Daria Sicari, Caterina Valetti, Edgar Djaha Yoboue, Tiziana Anelli, Roberto Sitia

anelli.tiziana@hsr.it (T.A.)
sitia.roberto@hsr.it (R.S.)

HIGHLIGHTS

ERGIC-53 binds ERp44 and accelerates its exit from the ER

Genetic or pharmacological inhibition of ERGIC-53 impairs ERp44 retrieval function

ERp44 and ERGIC-53 form a functional couple needed for post-ER QC

Tempio et al., iScience 24, 102244
March 19, 2021
https://doi.org/10.1016/j.isci.2021.102244

iScience

CellPress
OPEN ACCESS

Article

A virtuous cycle operated by ERp44 and ERGIC-53 guarantees proteostasis in the early secretory compartment

Tiziana Tempio,[1,2] Andrea Orsi,[1] Daria Sicari,[1,2,4] Caterina Valetti,[3] Edgar Djaha Yoboue,[1] Tiziana Anelli,[1,2,5,*] and Roberto Sitia[1,2,*]

SUMMARY

The composition of the secretome depends on the combined action of cargo receptors that facilitate protein transport and sequential checkpoints that restrict it to native conformers. Acting after endoplasmic reticulum (ER)-resident chaperones, ERp44 retrieves its clients from downstream compartments. To guarantee efficient quality control, ERp44 should exit the ER as rapidly as its clients, or more. Here, we show that appending ERp44 to different cargo proteins increases their secretion rates. ERp44 binds the cargo receptor ER-Golgi intermediate compartment (ERGIC)-53 in the ER to negotiate preferential loading into COPII vesicles. Silencing ERGIC-53, or competing for its COPII binding with 4-phenylbutyrate, causes secretion of Prdx4, an enzyme that relies on ERp44 for intracellular localization. In more acidic, zinc-rich downstream compartments, ERGIC-53 releases its clients and ERp44, which can bind and retrieve non-native conformers via KDEL receptors. By coupling the transport of cargoes and inspector proteins, cells ensure efficiency and fidelity of secretion.

INTRODUCTION

Eukaryotic cells must transport a wide variety of proteins to the extracellular space, plasma membrane, and organelles of the exocytic and endocytic compartments. These proteins translocate co-translationally into the endoplasmic reticulum (ER), where the sequential processes needed to reach their native conformation begin. Coupling efficiency and fidelity in protein secretion is key for professional secretory cells, which have to release huge amounts of proteins of high quality in a short time. The compartmentalized organization of the secretory pathway (ER, ER-Golgi intermediate compartment [ERGIC], and Golgi stacks) is important for guaranteeing efficiency in protein secretion. By placing folding chaperones and enzymes in different subregions, it ensures that proteins undergo the required post-translational modifications (i.e. glycosylation, oxidative folding, oligomerization) in the proper order. In parallel, regulated anterograde and retrograde vesicular transport systems maintain membrane homeostasis, allowing cargo receptors to cycle and facilitate the export of select clients. The selection of these "privileged" proteins depends on motifs that allow binding to cargo receptors in the ER and release in downstream compartments. Proteins devoid of positive transport signals are instead inserted into forward moving vesicles by default and hence move more slowly following bulk flow (Barlowe and Helenius, 2016; Barlowe and Miller, 2013).

While the above systems promote forward transport, sequential quality control (QC) mechanisms guarantee secretome fidelity, retaining non-native conformers in the ER or retrieving them from downstream compartments. Parallel networks of ER-resident proteins (i.e. GRP78/BiP, GRP94, CNX, CRT, PDI) prevent the exit from the ER of misfolded or unassembled proteins by active retention (Anelli and Sitia, 2008; Molinari and Helenius, 1999; Sun and Brodsky, 2019). ERp44, a folding assistant of the PDI family (Anelli et al., 2002, 2003), operates instead a distal QC checkpoint, retrieving a select protein clientele from downstream compartments. Unlike BiP, PDI, CRT, and other ER-residents involved in proximal QC, ERp44 is found also in ERGIC and cis-Golgi (Anelli et al., 2007). Its functional cycle is controlled by pH- and zinc-dependent conformational changes (Vavassori et al., 2013; Watanabe et al., 2017, 2019). At the neutral pH of the ER, ERp44 adopts a compact conformation, in which neither the client binding site nor the C-terminal RDEL motif is accessible. In the acidic and zinc-rich milieu of ERGIC and cis-Golgi, however, ERp44 undergoes conformational changes that allow the capture of client proteins. These

[1]Division of Genetics and Cell Biology, IRCCS San Raffaele Scientific Institute, 20132 Milan, Italy

[2]Vita-Salute San Raffaele University, 20132 Milan, Italy

[3]Department of Experimental Medicine, University of Genoa, 16132 Genoa, Italy

[4]Present address: IFOM, Fondazione Istituto FIRC di Oncologia Molecolare, Milan, Italy

[5]Lead contact

*Correspondence: anelli.tiziana@hsr.it (T.A.), sitia.roberto@hsr.it (R.S.)

https://doi.org/10.1016/j.isci.2021.102244

include enzymes that act primarily in the ER but lack KDEL-like motifs (i.e. Ero1, Prdx4, Sumf1/FGE1, ERAP1), as well as incompletely assembled cargoes, including IgM, adiponectin, and IL-23 (Anelli et al., 2007; Hampe et al., 2015; Meier et al., 2019; Tempio and Anelli, 2020). ERp44 binds its substrates covalently, via its cysteine 29 (Anelli et al., 2003; Watanabe et al., 2017; Yang et al., 2016). Not only does the opening of the ERp44 C-terminal tail allow substrate binding but it also exposes its RDEL motif, allowing KDEL receptors (KDELR) to bind and retrieve ERp44-substrate complexes. Upon retrieval, clients are likely released in the neutral (Miesenböck et al., 1998; Vavassori et al., 2013) and low zinc (Kambe et al., 2017; Kowada et al., 2020; Qin et al., 2011) ER environment following PDI-dependent reduction (Yang et al., 2016).

To guarantee efficient post-ER QC, mechanisms are likely to operate ensuring that ERp44 outnumbers its clients in ERGIC and cis-Golgi. The different distribution of ERp44 with respect to most ER residents endowed with KDEL-like motifs implies that additional mechanisms determine the localization of soluble chaperones and enzymes, besides KDELR-dependent retrieval (Munro and Pelham, 1987). BiP, PDI, GRP94, CaBP1, UGGT1, and other ER residents form multi-molecular complexes, the diffusibility of which is further reduced by unfolded proteins (Costantini and Snapp, 2013; Meunier et al., 2002; Reddy et al., 1996; Snapp et al., 2006). Not being part of these complexes, ERp44 can move more freely. Accordingly, a variant lacking the RDEL motif, ERp44ΔRDEL, is secreted faster than a corresponding PDI mutant (Anelli et al., 2007). Also interactions with specific cargo receptors might facilitate transport to downstream compartments (Appenzeller-Herzog et al., 2004; D'Arcangelo et al., 2013; Herzig et al., 2012; Kuehn et al., 1998; Mitrovic et al., 2008; Raote et al., 2018). A possible factor favoring forward ERp44 transport is ERGIC-53: this hexameric lectin acts as a cargo receptor facilitating the export from the ER of glycoprotein substrates, such as factors V and VIII of the coagulation cascade, α1 antitrypsin, and IgM (Anelli et al., 2007; Hauri et al., 2000; Zhang et al., 2009). ERGIC-53 recycles continuously between the ER and the cis-Golgi, thanks to interactions of its cytosolic C-terminal KKFF motif with COPI (KK) and COPII (FF) (Appenzeller et al., 1999; Wendeler et al., 2007). ERGIC-53 binds its cargoes in the ER, releases them in the acidic cis-Golgi, and goes back to the ER to start a new cycle. Thus, ERGIC-53 activity is regulated in an opposite way with respect to ERp44 (Tempio and Anelli, 2020).

We reasoned that ERp44 could exploit ERGIC-53 to reach downstream compartments and ensure distal QC. To provide evidence for this model, we compared the localization and secretory rates of a panel of ERp44 chimeras or suitably engineered reporter proteins. We also analyzed the secretion of different ERp44 clients upon genetic or pharmacologic ERGIC-53 inhibition. Our results show that ERGIC-53-driven transport of ERp44 is crucial to ensure efficient post-ER protein QC.

RESULTS

ERp44 contains information that promotes its export from the ER

To investigate whether ERp44 contains positive transport signals, we appended ERp44ΔRDEL to the C-terminal end of three different cargo proteins: (1) the bacterial enzyme Halo carrying the ERp44 signal peptide at its N-terminus (spHalo-44ΔRDEL); (2) a secretion competent Ig-λ light chain (Igλ-44ΔRDEL); (3) an ER-localized GFP (spGFP-44ΔRDEL) (Figures 1 and S1). Care was taken to remove the C-terminal cysteine of Ig-λ, which acts as a weak retention signal and mediates reversible Ig-λ interaction with ERp44 (Anelli et al., 2003; Reddy et al., 1996). Marked differences were evident when we compared the secretion rates of the cargo chimeras carrying the ERp44ΔRDEL moiety and cargo alone. In all three cases, the chimeric proteins disappeared from the intracellular pool and were secreted much faster than their counterparts lacking ERp44 (Figures 1A, 1B, and S1). Similar findings were obtained by radioactive pulse-chase assays for the spHalo and spHalo-44ΔRDEL proteins (Figure S2A).

We then settled on spHalo and spHalo-44ΔRDEL as the more convenient secretion reporters. The use of Halo has multiple advantages. First, it allows monitoring the folding state of the molecule, as only if properly folded Halo can bind its ligand. Second, distinct Halo ligands are available that carry different fluorescent moieties. Since the binding of Halo to its ligand is irreversible, this allows us to label proteins in a precise moment and to follow that protein population in time (visual pulse-chase assay). Finally, considering its bacterial origin, Halo is unlikely to have coevolved with effectors in the mammalian secretory protein factory and it could hence be considered a bona fide neutral reporter of bulk flow transport (Mossuto et al., 2014; Thor et al., 2009).

The different secretion rates correlated with different intracellular localization of the two molecules. At steady state, spHalo displayed an intense reticular distribution, while spHalo-44ΔRDEL showed negligible co-localization with calreticulin (CRT) and instead accumulated in ERGIC and cis-Golgi vesicles (Figure 1C). To visualize their movement, we took advantage of Halo's properties and set up visual pulse-chase assays. First, we saturated all pre-existing molecules with an unlabeled ligand; then, we labeled those synthesized in a 20-min pulse with a fluorescent ligand and eventually chased them in the presence of the unlabeled ligand and puromycin. As shown in Figure 1E, at the beginning of chase, spHalo is mostly found in the ER, as revealed by co-localization with CRT (Figure S2B) and its absence from GM130-positive structures. In contrast, in agreement with its faster secretion, spHalo-44ΔRDEL shows already extensive co-localization with GM130 (compare yellow color in the merge panels). After 1 hr of chase, when spHalo is reaching the Golgi, spHalo-44ΔRDEL has already started to move out of the compartment and accumulate in secretory vesicles. After 2 hr of chase, there is virtually no spHalo-44ΔRDEL left in the Golgi, while spHalo is lagging behind.

Altogether, these data show that appending ERp44 to a bulk flow reporter confers features that facilitate anterograde traffic along the secretory pathway. Thus, ERp44 promotes the transport of different proteins, independently from their properties and basal secretory rates.

The lectin ERGIC-53 facilitates the exit of ERp44 from the ER

Interactions with the cargo receptor ERGIC-53 (Anelli et al., 2007) would explain the rapid movement of ERp44 containing chimeras. Accordingly, we found that ERGIC-53 specifically co-precipitates with spHalo-ERp44 (Figure 2A, red arrow) but not with spHalo (Figure 2A). The interaction between ERp44 and ERGIC-53 occurs also in physiological conditions: indeed in mock-transfected cells anti-ERp44 antibodiesco-precipitated endogenous ERGIC-53 (Figure 2B; lanes 1, 2, 3). The association was more evident in cells co-expressing GM-ERGIC-53, an N-glycosylated, myc-tagged ERGIC-53 variant (Appenzeller et al., 1999), and either HA-ERp44 (lanes 5, 6, 7) or Halo-ERp44 (lanes 8, 9, 10). These results exclude a role of the tags in mediating the interactions between ERGIC-53 and ERp44.

To determine whether ERGIC-53 favors the exit of ERp44 from the ER, we exploited a non-radioactive pulse-chase assay to compare the fate of spHalo-44ΔRDEL and spHalo molecules upon ERGIC-53 silencing (Figure 3A). Aliquots of the lysates and supernatants were resolved electrophoretically and the Halo/TMR (tetramethylrhodamine) fluorescent signals detected in gels (panel A) were quantified by densitometry (panel B). As expected, the intracellular signal decreased over time, accumulating extracellularly for both proteins.

Also with this assay, in untreated cells, the kinetics of secretion were faster for spHalo-44ΔRDEL than for spHalo (Figure 3B, compare red and blue lines). A considerable fraction of spHalo remained within cells after two hours of chase, when the majority of spHalo-44ΔRDEL had been exported. Importantly, the down-regulation of ERGIC-53 (Figure 3A, right panels) slowed down the export of spHalo-44ΔRDEL (compare dark and light red lines in Figure 3B) but had no detectable effects on spHalo (dark and light blue lines).

Thus, anterograde transport of ERp44 is facilitated by ERGIC-53 and downregulation of the lectin attenuates the differences in the secretion rate between spHalo and spHalo-44ΔRDEL. Such difference is not completely abolished by ERGIC-53 silencing, however, suggesting that either the few residual ERGIC-53 molecules are still able to assist spHalo-44ΔRDEL export or that ERGIC-53 is not the sole system promoting ERp44 cycling. Radioactive pulse-chase experiments confirmed that ERGIC-53 assists the export of ERp44 (Figures S3A and S3B).

Taken together, the above results show that, thanks to its association with ERGIC-53, ERp44 exits the ER faster than a bulk flow reporter.

ERGIC-53 mediates ERp44 export via COPII vesicles

To gain insight into the mechanisms that facilitate the export of ERp44, we sought to impair the exit of ERGIC-53 from the ER, a process that is mediated by the recognition of the FF export signal present on ERGIC-53 by Sec24, a component of the inner COPII coat. Human cells express four Sec24 isoforms that are functionally redundant (Wendeler et al., 2007). Among them, isoforms A and B have been described to be important for ERGIC-53 FF-mediated ER export (Nufer et al., 2003; Wendeler et al., 2007; Zeyen et al., 2020). However, in our hands, the double (A and B) or multiple knockdowns of Sec24 isoforms had only

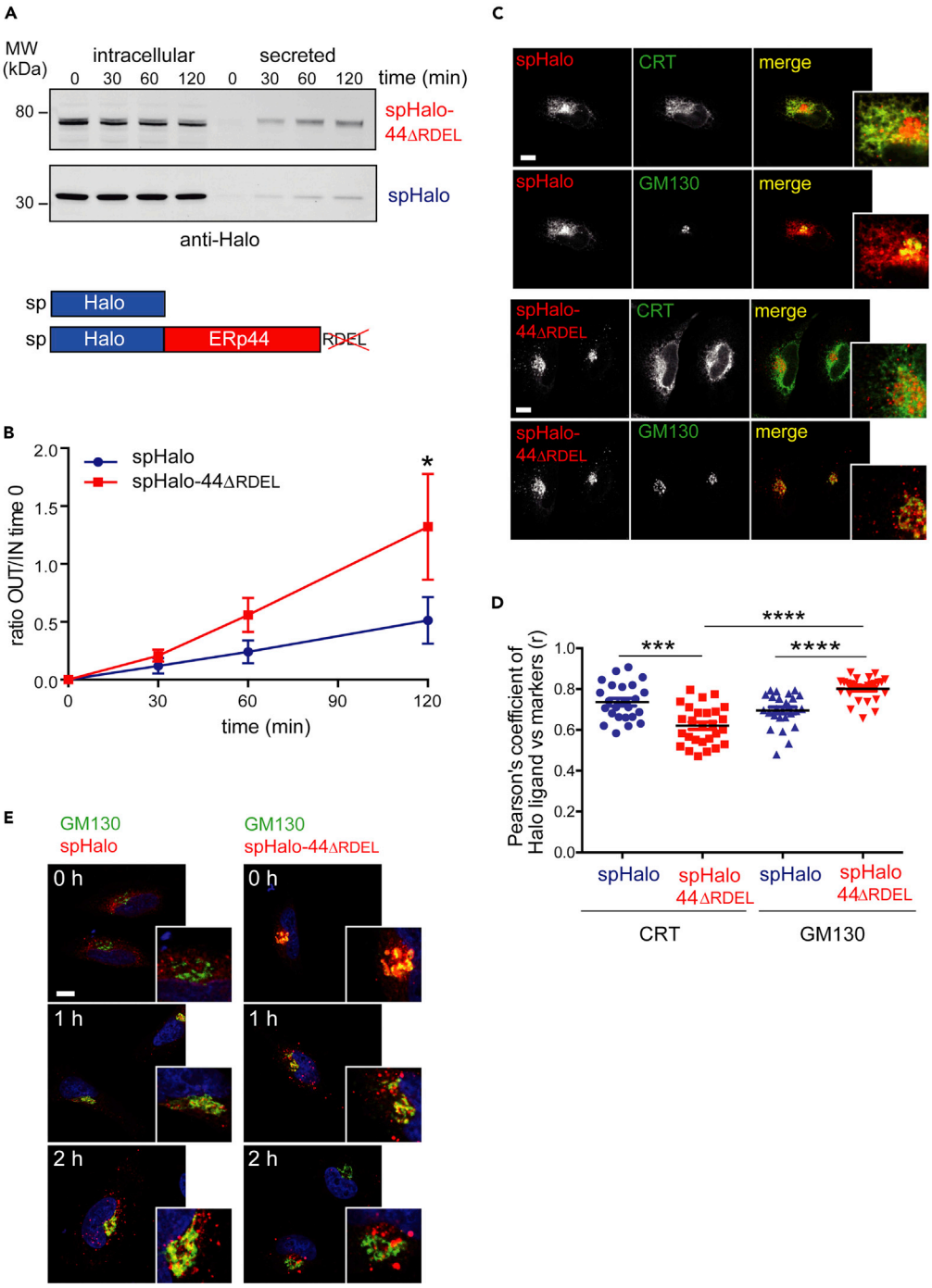

Figure 1. Appending a secretable ERp44 facilitates secretion of neutral cargo

(A) The lysates (intracellular) and supernatants (secreted) of spHalo-44ΔRDEL and spHalo HeLa transfectants cultured in the presence of puromycin were collected at the indicated time points and aliquots (corresponding to $2*10^5$ cells) resolved by reducing SDS-PAGE (sodium dodecyl (lauryl) sulfate-polyacrylamide gel electrophoresis). In the experiment shown, blots were decorated with anti-Halo antibodies. spHalo-44ΔRDEL is secreted faster than spHalo, appearing sooner in the supernatants. The slower gel mobility of secreted spHalo-44ΔRDEL with respect to the intracellular protein reflects ERp44 O-glycosylation (Sannino et al., 2014). O-glycosylated precursors are detected also in the lysates of spHalo-44ΔRDEL . See also Figures S1 and S2.

Figure 1. *Continued*

(B) Secretion rates were calculated by densitometric quantification of the extracellular bands relative to the corresponding intracellular signals at time zero. Average of four independent experiments like the one shown in A, +/− SEM (standard error of the mean). Statistical analysis was performed using t test.

(C) HeLa transfectants expressing spHalo or spHalo-44ΔRDEL were incubated for 2 hr with TMR (tetramethylrhodamine) Halo ligand and then fixed and labeled with anti-CRT and anti-GM130 antibodies in combination. To better appreciate the different distribution of spHalo and spHalo-44ΔRDEL, the same image for TMR signal (red) is shown twice and overlaid with either CRT or GM130 signals pseudo-colored in green. Unlike spHalo, spHalo-44ΔRDEL localizes at the ER only in minimal part and instead is more abundant in downstream compartments. Scale bar, 10 μm in all images. In zoom panels, regions of interest are magnified 2.9 folds. Over 25 cells were analyzed in detail for each transfectant in two independent experiments.

(D) Pearson's correlation coefficient analysis. Statistical analysis was performed using Mann-Whitney test.

(E) Newly synthesized spHalo-44ΔRDEL or spHalo molecules were labeled with TMR Halo ligand for 20 min as detailed in the text (visual pulse-chase assay). Cells were then cultured in the presence of unlabeled Halo ligands and puromycin and analyzed by fluorescence microscopy at the indicated times. A merged image with Halo-tagged proteins in red, Golgi marker GM130 in green, and nuclei in blue is shown. The earlier appearance of spHalo-44ΔRDEL in the Golgi area and its subsequent disappearance correlate with the faster secretion kinetics. Zoom panels are magnified 2.4 folds. At least 20 cells were analyzed at each time point in 3 independent experiments; representative images are shown in the panels. See also Figure S2.

minor effects on ERp44 transport (data not shown). Real-time analyses of mRNA transcripts in HeLa cells, which express constitutively all four Sec24 isoforms, suggested possible compensatory effects of individual subunits when others have been acutely silenced (Wendeler et al., 2007 and our unpublished data). To circumvent this problem, we exploited 4-phenylbutyrate (4-PBA), a drug that has been shown to occupy the Sec24 groove that normally accepts the FF motif of ERGIC-53. In this way, 4-PBA inhibits COPII-mediated transport of the lectin and other FF-driven cargo receptors (Ma et al., 2017). Acute inhibition during the short time of the experiment limits the confounding compensatory effects that are often induced by knockdown or knockout experiments. Strikingly, 4-PBA treatment blunted almost completely spHalo-44ΔRDEL secretion (Figure 4). The drug did not inhibit bulk flow secretion but rather slightly increased spHalo (compare light blue with dark dashed blue lines, Figure 4B). The above data confirm that ERp44 binds ERGIC-53 in the ER and proceeds toward the Golgi via COPII. The selective inhibition of spHalo-44ΔRDEL exerted by 4-PBA likely reflects prolonged interactions with ERGIC-53 and other receptors normally exported by Sec24.

ERGIC-53 favors the interactions of ERp44 with its clients

The above results suggested that ERGIC-53 allows ERp44 to reach ERGIC and cis-Golgi in adequate amounts to perform its retrieval function. We hence surmised that in the absence of ERGIC-53, secretion of ERp44 clients would be favored. To test this hypothesis, we analyzed the fate of peroxiredoxin 4 (Prdx4), an enzyme that lacks a KDEL-like motif and is retrieved from the ER by ERp44 (Kakihana et al., 2013; Otsu et al., 2006; Yang et al., 2016). Prdx4 carries no N-glycans, and hence, it cannot bind to the ERGIC-53 carbohydrate recognition domain. As previously observed, ERp44 silencing facilitated secretion of endogenous Prdx4. Also, ERGIC-53 downregulation or 4-PBA administration promoted Prdx4 secretion, confirming our hypothesis (Figure 5). These data indicate that the role of ERGIC-53 in promoting ERp44 exit from the ER is crucial to ensure efficient ERp44-dependent QC. As previously described (Ma et al., 2017), the drug induced secretion of KDEL proteins, recognized by anti-KDEL antibodies, approximately at 90 kDa (likely GRP94, panel A). Also, ERp57 is secreted (panel D). Thus, the slightly stronger effects of 4-PBA in inducing Prxd4 secretion compared to ERp44 or ERGIC-53 silencing could reflect a general weakening of transport selectivity. Next, we performed similar experiments with Sumf1/FGE. Differently from Prdx4, this enzyme is N-glycosylated and is a client of both ERGIC-53 and ERp44 (Fraldi et al., 2008; Mariappan et al., 2008). As expected, Sumf1 was secreted faster upon ERp44 downregulation. Differently from Prdx4 and consistent with the fact that ERGIC-53 favors Sumf1 export (Fraldi et al., 2008), silencing the lectin or adding 4-PBA had lower but detectable effects on Sumf1 release, indicating that the ERp44-dependent retrieval plays a greater role than ERGIC-53 in determining the localization of Sumf1.

Zinc-dependent regulation of ERGIC-53 localization via ERp44

The fact that spHalo-44ΔRDEL is rapidly secreted implies that, despite its interactions with ERGIC-53 during export from the ER, it eventually detaches from the lectin in downstream compartments. ERGIC-53 and ERp44 are known to undergo pH-dependent conformational changes (Appenzeller-Herzog et al., 2004;

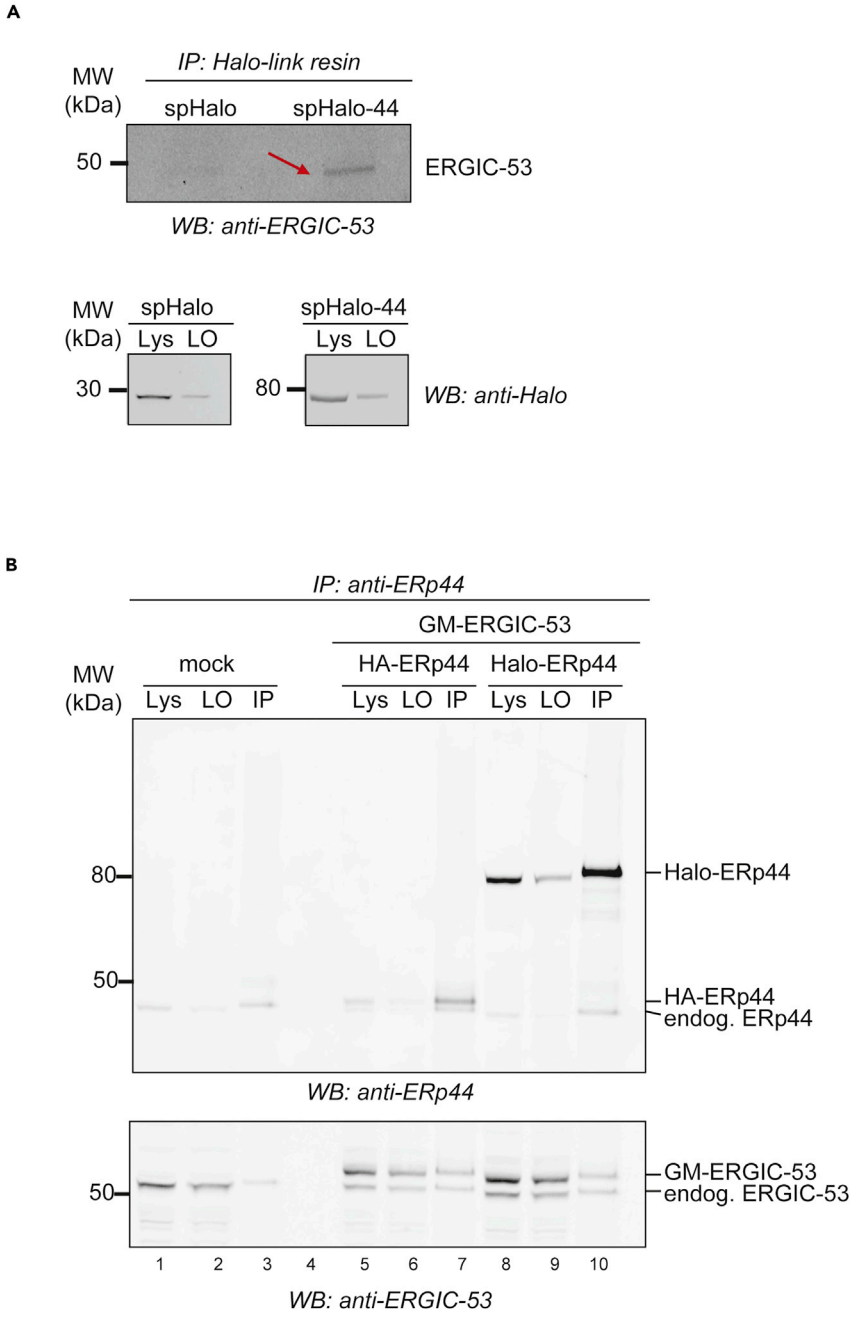

Figure 2. The lectin ERGIC-53/LMAN1 binds to ERp44

(A) Aliquots (1 mg of total proteins) of lysates of spHalo-44 or spHalo expressing HeLa transfectants were precipitated with immobilized Halo ligands. Proteins associated to Halo-tagged baits were eluted in Laemli buffer and resolved by SDS-PAGE (sodium dodecyl (lauryl) sulfate-polyacrylamide gel electrophoresis) under reducing conditions. Blots were decorated with anti-ERGIC-53 antibody, as indicated. Endogenous ERGIC-53 (red arrow) specifically interacts with spHalo-44 but not with spHalo (upper panel). The bottom panels show the precipitation efficiency.

(B) Aliquots from the lysates of HeLa cells transfected or not with GM-ERGIC-53 and Halo-ERp44 or HA-ERp44 were immunoprecipitated with immobilized anti-ERp44 antibodies, and the immunoprecipitated material was resolved by SDS-PAGE under reducing conditions. Lysates and leftover (LO) corresponding to 20 μg of proteins were loaded; IP (immunoprecipitation) was performed on 500 μg of total protein lysates. Blots were decorated with anti-ERGIC-53 and anti-ERp44 antibodies. ERGIC-53 and ERp44 interact independently from the presence of tags on the two proteins.

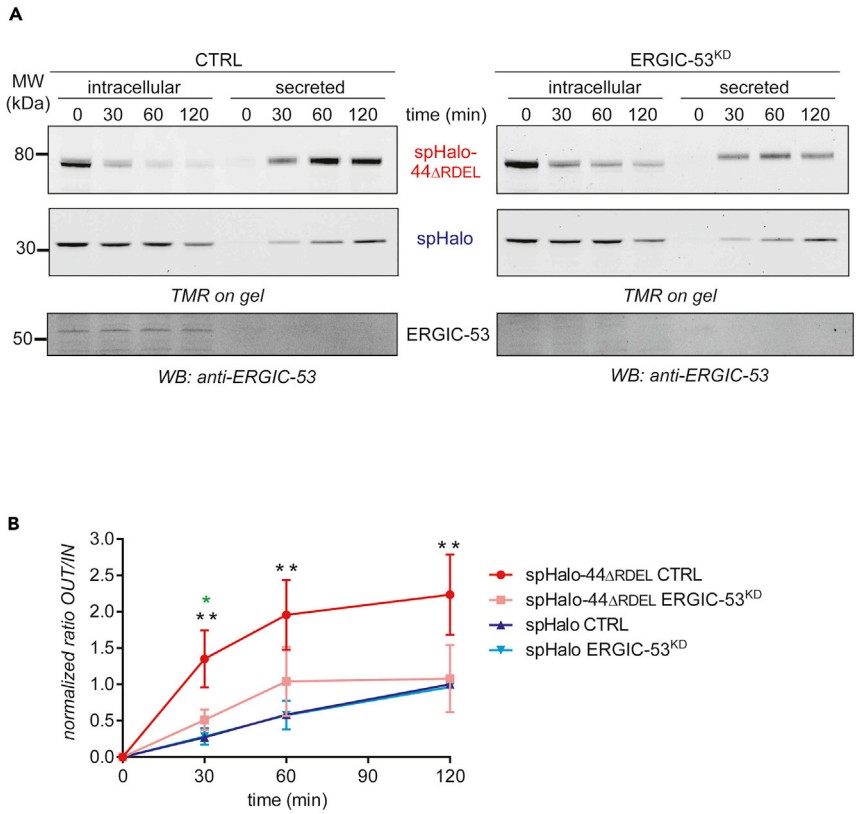

Figure 3. ERGIC-53 depletion specifically reduces spHalo44-ΔRDEL secretion

(A) HeLa cells were silenced with specific (ERGIC-53^{KD}) or control (CTRL) oligos as indicated and forced to transiently express spHalo-44ΔRDEL or spHalo. Forty-eight hrs after transfection, cells were incubated with an unlabeled Halo ligand, washed thoroughly, labeled for 20 min with fluorescent TMR Halo ligand, washed again, and incubated for the indicated times in the presence of unlabeled Halo ligands and puromycin. Aliquots of intracellular and secreted material corresponding to 2*10^5 cells were resolved electrophoretically under reducing conditions, and gels were directly analyzed by fluorography. Note that secreted spHalo-44ΔRDEL is O-glycosylated, excluding passive release (top). Bottom panels confirm the efficiency of ERGIC-53 silencing.

(B) The graph shows the densitometric quantification of several independent experiments like the one showed in (A). The ratio secreted/intracellular TMR-labeled signals was calculated for each time point. Then, all values were normalized to the ratio obtained for spHalo CTRL at 120 min time point, assumed to represent the secretion of a bulk flow protein in each experiment. The averages of n experiments +/− SEM (standard error of the mean) (n = 5 for spHalo-44ΔRDEL and for spHalo CTRL, n = 4 for spHalo-44ΔRDEL ERGIC-53^{KD}, n = 2 for spHalo ERGIC-53^{KD}) are plotted in the graph. Statistical analysis was performed using non-parametric Mann-Whitney test; **p < 0.007; *p < 0.03. The black and green asterisks are referred to the comparison of spHalo-44ΔRDEL with spHalo CTRL and spHalo-44ΔRDEL ERGIC-53^{KD}, respectively. These experiments demonstrate that ERGIC-53 silencing selectively slows down spHalo-44ΔRDEL secretion, without any effect on spHalo secretion.

See also Figure S3.

Watanabe et al., 2017) and so do KDELR (Bräuer et al., 2019; Wilson et al., 1993; Wu et al., 2020). Also, zinc regulates the localization, conformation, and activity of ERp44, allowing client and KDELR binding (Watanabe et al., 2019). As previously observed, chelating zinc using a membrane-permeable ion chelator (TPEN) caused the accumulation of ERp44 in the Golgi area; interestingly, ERGIC-53 adopted a similar distribution upon TPEN treatment (Figure 6A, middle panels and Figure S4A). *Vice versa*, upon addition of $ZnCl_2$, both ERp44 and ERGIC-53 displayed a diffuse reticular pattern consistent with their retrieval to the ER (Figure 6A, bottom panels and Figure S4A). These analyses were performed in both T-HESC, a physiological model of secretory cells (Krikun et al., 2004), and HeLa cells. Importantly, the localization of ERGIC-53 was not altered by zinc modulation in cells lacking ERp44 (Figure 6B), demonstrating that ERGIC-53 itself is insensitive to zinc and its re-localization depends on the presence of ERp44. In the short time frame of these experiments, the addition and removal of zinc did not alter significantly the distribution of GM130, a cis-Golgi marker (Figure 6B). As zinc favors the KDELR-dependent retrieval of ERp44 (Watanabe et al., 2019), ERGIC-53

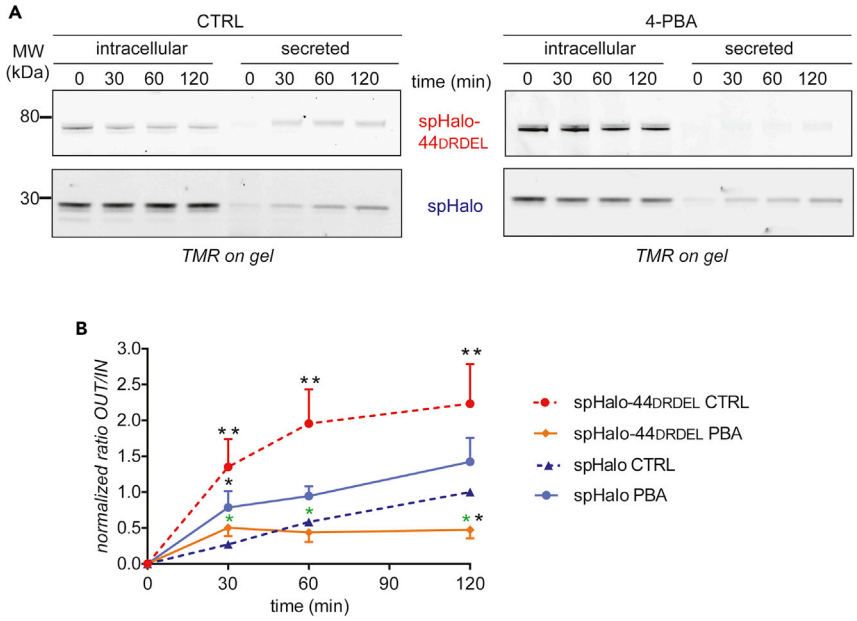

Figure 4. 4-PBA selectively prevents spHalo-44ΔRDEL secretion

(A) HeLa cells were treated as in Figure 3, with the exception that 48 hr after transfection, part of the cells were pre-treated for 2 hr with 4-PBA (10 mM). For these samples, 4-PBA was kept also during the pulse and the chase. Aliquots of intracellular and secreted material corresponding to $2*10^5$ cells were resolved electrophoretically, and gels were directly analyzed by fluorography as in Figure 3.

(B) The graph shows the densitometric quantification of independent experiments (n = 5 for spHalo-44ΔRDEL CTRL, n = 5 for spHalo CTRL, n = 3 for spHalo-44ΔRDEL 4-PBA, n = 3 for spHalo 4-PBA) like the one displayed in (A). Quantification was performed as described in legend to Figure 3B.

Statistical analysis was performed using non-parametric Mann-Whitney test; **p < 0.007; *p < 0.03; the black asterisks are referred to the comparison to spHalo CTRL; the green asterisks are referred to the comparison to spHalo-44ΔRDEL CTRL. The dashed red and blue lines are the same (respectively red and blue) shown in Figure 3, reported here to facilitate the comparison among different experiments. Notably, 4-PBA selectively inhibits spHalo-44ΔRDEL secretion, slightly inducing spHalo release.

re-localization could depend on augmented membrane retrieval to the ER. Alternatively, zinc might inhibit the exit of ERGIC-53 from the ER destabilizing its association with ERp44. In support of the latter mechanism, ERGIC-53 displays a reticular pattern in ERp44^{KD} cells (Figure 6B top panel and Figure S4B). Taken together, these results strengthen the idea that ERp44 and ERGIC-53 not only interact and travel together in the early secretory compartment but also mutually co-regulate each other's cycling.

DISCUSSION

Retention of a protein in the ER can be caused by either its association to chaperone complexes with low diffusibility (Borgese et al., 2006; Costantini and Snapp, 2013; Lai et al., 2010; Meunier et al., 2002; Reddy et al., 1996) or by exclusion from forward moving vesicles because of competition with other proteins for cargo receptors (Borgese, 2016; Ma et al., 2017). Retrieval, instead, depends on ERp44 and other chaperones that—unlike ER-resident ones—bind clients in downstream compartments (Shibuya et al., 2015; Sun and Brodsky, 2019; Anelli and Sitia 2008) and transport them backwards to the ER. This stepwise QC is important for the manufacture of complex proteins (Hampe et al., 2015; Meier et al., 2019; Tempio and Anelli, 2020). Our findings show how ERp44 reaches distal compartments in sufficient amount to capture all clients needing retrieval. By reversibly associating with cargo receptors that cycle in the early secretory compartment, ERp44 can proceed faster than bulk flow proteins, thus outnumbering its substrates.

The faster secretion of three different chimeric proteins upon extension with ERp44ΔRDEL indicates that ERp44 contains properties that facilitate its exit from the ER. One is the low affinity with the ER matrix (Meunier et al., 2002). Another is its ability to bind ERGIC-53. Indeed, silencing ERGIC-53 slows down secretion

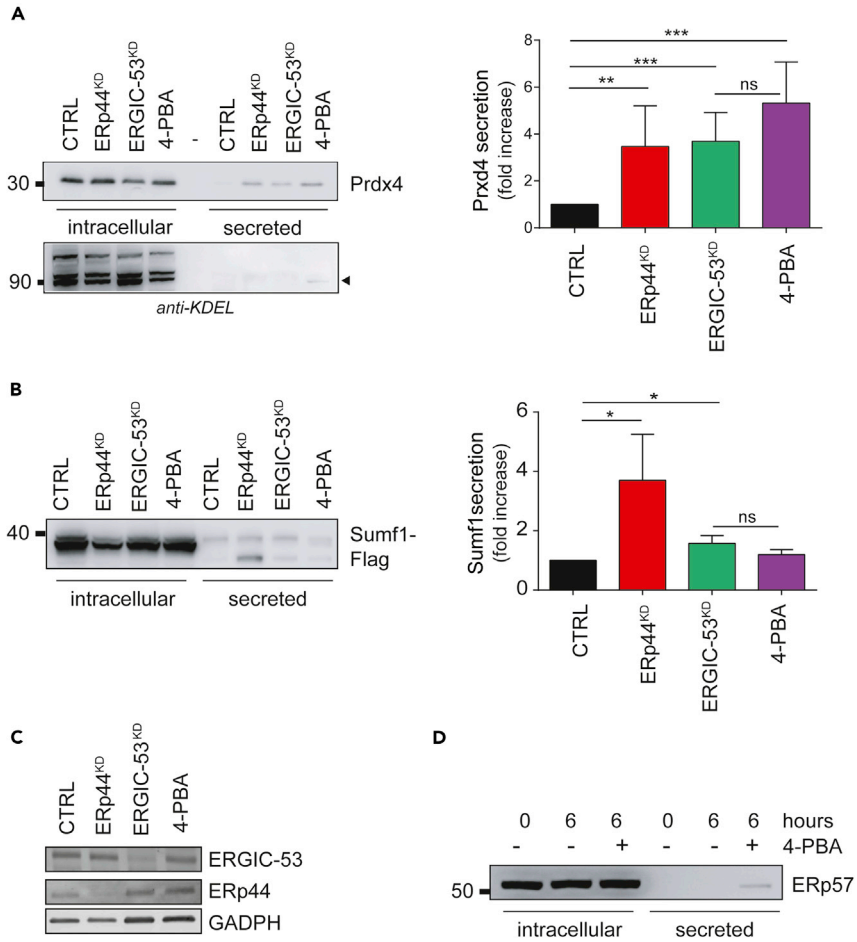

Figure 5. Genetic or pharmacologic knockdown of ERGIC-53 weakens ERp44-dependent, post-ER quality control

HeLa cells, silenced or treated as indicated, were washed and incubated in Opti-MEM supplemented with or without 4-PBA (10 mM) for 4 hr, unless otherwise indicated. The lysates of $2x10^5$ cells (intracellular) and the supernatants corresponding to $1x10^6$ cells (secreted) were collected. After supernatant concentration, both were resolved by reducing SDS-PAGE (sodium dodecyl (lauryl) sulfate-polyacrylamide gel electrophoresis), followed by immunoblotting with the indicated antibodies.

(A) Secretion of Prdx4 is promoted by downregulation of either ERp44 or ERGIC-53 and by 4-PBA. The graph shows the fold increase of secreted/intracellular ratio band relative to untreated cells. Average of 6 independent experiments +/− SEM (standard error of the mean). Statistical analysis was performed using unpaired t test. **$p < 0.005$; ****$p < 0.0001$. Hybridization of the upper region of the same filter with anti-KDEL antibodies reveals secretion of a band of approximately 90–95 kDa upon 4-PBA treatment. The absence of signal in correspondence of the other bands, abundant intracellularly, confirms the specificity of the silencing or 4-PBA effects.

(B) Secretion of FLAG-tagged Sumf1 is promoted by downregulation of ERp44 and to a lesser extent of ERGIC-53. The faster migrating band accumulating extracellularly likely represents a truncated Sumf1 isoform. The graph derives from the quantification of 6 different experiments. Statistical analysis was performed using unpaired t test. *$p < 0.01$. Proteasome inhibitors were added during this experiment to prevent degradation of Sumf1 (Fraldi et al., 2008). Hybridization with anti-KDEL or Prxd4 antibodies yielded results to those shown in (A), excluding unexpected artifacts of proteasome inhibitors.

(C) Silencing efficacy was confirmed by immunoblotting.

(D) Some ERp57 is secreted upon 4-PBA treatment.

of spHalo-44ΔRDEL, without affecting spHalo. Associations with Sec24 facilitate the insertion of ERGIC-53 into COPII vesicles (Nufer et al., 2003). In our hands, silencing Sec24 isoforms individually or in combinations had only partial effects (not shown), likely also owing to the redundancy (and robustness) of forward transport systems (Wendeler et al., 2007). However, we obtained clear-cut results with 4-PBA, a drug originally developed as a chemical chaperone to combat cystic fibrosis (Rubenstein and Zeitlin, 1998) and

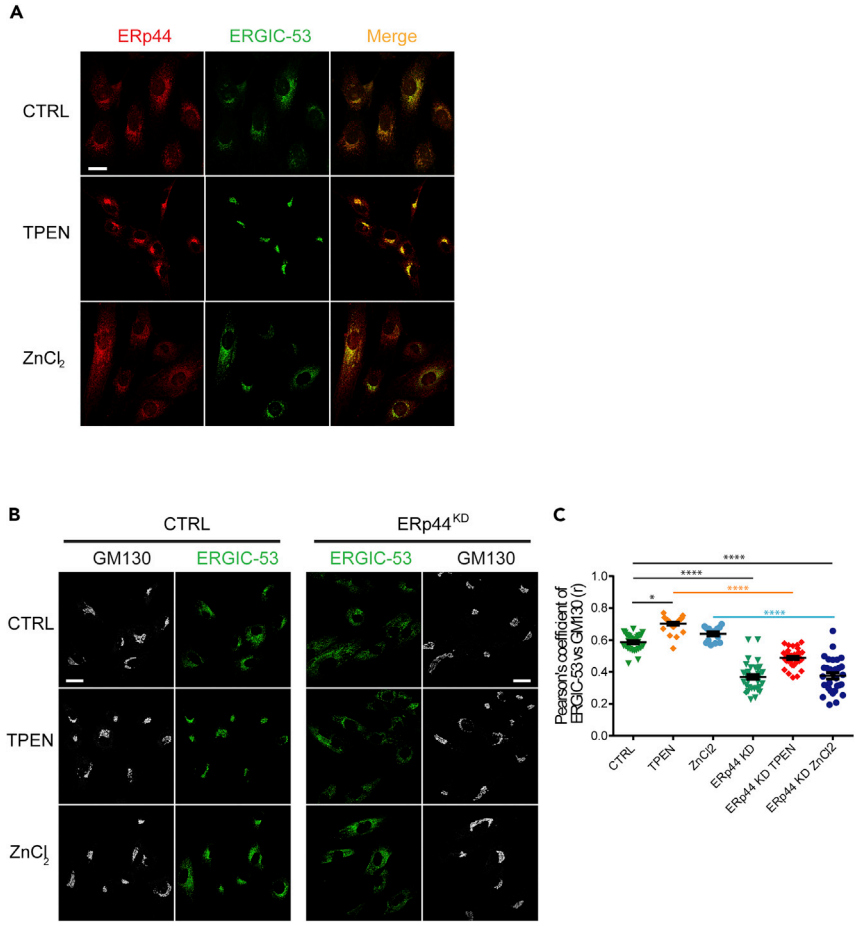

Figure 6. Zinc indirectly modulates ERGIC-53 localization via ERp44

(A) Immortalized human endometrial stromal cells (T-HESC) were cultured with TPEN (30 min) or $ZnCl_2$ (3 hr), fixed, permeabilized and analyzed by immunofluorescence with ERGIC-53- or ERp44-specific antibodies. Note the colocalization between ERp44 (red) and ERGIC-53 (green), both accumulating in the Golgi in the absence of zinc (middle panels) or showing a reticular pattern upon zinc addition (lower panels). Scale bar, 20 μm. More than 30 cells for each condition were analyzed in detail in two independent experiments.

(B) T-HESC cells were silenced with control (CTRL) or ERp44 ($ERp44^{KD}$)-specific duplexes and treated as above. Note that ERGIC-53 is almost insensitive to changes in zinc concentration when ERp44 is absent (compare ERGIC-53 signal, in green, upon CTRL, TPEN, and $ZnCl_2$ treatments). The cis-Golgi pattern structure is not grossly affected by zinc modulation (compare GM130 signal, in white, upon CTRL, TPEN, and $ZnCl_2$ treatments). Scale bar, 20 μm.

(C) Quantitative analyses of Pearson's correlation coefficients of ERGIC-53 with GM130 are shown in the graph on the right. Dots indicate individual cells (>15 cells from 2 independent experiments). Statistical analysis was performed using Kruskall-Wallis test (*$p < 0.01$; **$p < 0.001$; ***$p < 0.001$).

See also Figure S4.

recently shown to compete with the di-phenylalanine motif of ERGIC-53 and other recycling molecules for Sec24 binding (Ma et al., 2017). As expected, 4-PBA selectively slowed down spHalo-44ΔRDEL, without affecting spHalo. Unexpectedly, spHalo-44ΔRDEL was secreted even less than the bulk flow reporter in the presence of the drug. Thus, 4-PBA not only counteracted the preferential export of spHalo-44ΔRDEL but also caused its selective retention, likely retaining ERGIC-53 in proximal compartments where the association with ERp44 is promoted.

Many lines of evidence indicate that ERp44 binds ERGIC-53 in the ER. We previously showed that expression of a mutant ERGIC-53 lacking the FF motif for Sec24 binding retains ERp44 in the ER (Anelli et al., 2007). In this compartment, ERp44 adopts a compact, "closed" conformation, not suited for binding cargoes with high affinity (Vavassori et al., 2013; Watanabe et al., 2017, 2019; Yang et al., 2016), while ERGIC-53 is in

the ON mode for binding its client glycoproteins (Appenzeller et al., 1999; Zhang et al., 2009). Carrying no N-glycans, ERp44 likely interacts with ERGIC-53 outside the lectin-binding site: accordingly, it interacts also with an ERGIC-53 mutant unable to interact with glycoproteins (Cortini and Sitia, 2010). The rapid secretion of ERp44ΔRDEL implies that ERp44 dissociates from ERGIC-53 in downstream compartments, possibly due to the conformational changes that both interactors experience in the more acidic, zinc-rich Golgi milieu (Appenzeller-Herzog et al., 2004; Watanabe et al., 2019). Albeit specific, the interaction involves a minor fraction of the two molecules at steady state (Figure 2). This is hardly surprising, considering that the interaction must be easily reversed in downstream compartments. Clearly, further biochemical and structural studies are needed to decipher the structural and dynamic details of the ERp44/ERGIC-53 liaison.

Not only does ERGIC-53 influence the intracellular localization of ERp44, but also the reverse is true. ERGIC-53 displays a more reticular pattern in ERp44^{KD} cells (Figures 6B and S4B), suggesting that binding to ERp44 facilitates recruitment of ERGIC-53 into COPII vesicles. Moreover, changes in the concentration of zinc, known to induce the accumulation of ERp44 in the cis-Golgi or in the ER (Watanabe et al., 2019), cause the re-localization of ERGIC-53 in the same compartments. This is not a consequence of a direct dependency of ERGIC-53 to zinc: its intracellular localization is not affected by zinc in ERp44^{KD} cells (Figure 6B). The notion that ERp44 and ERGIC-53 display similar temporal expression patterns during B-cell differentiation and co-localize in most cell types (Anelli et al., 2007; Gilchrist et al., 2006; Figures 6A and S4A) reinforces the idea that they are part of a functional cycle.

The rapid exit of ERp44 is important for efficient client retrieval. ERGIC-53 silencing or 4-PBA administration induces secretion of endogenous Prdx4—a protein that lacks N-glycans and is retrieved by ERp44 (Kakihana et al., 2013; Otsu et al., 2006)—to a similar if not greater extent than downregulating the retriever itself. We interpret this finding to indicate a retarded arrival of ERp44 to its working compartments. Without the assistance of ERGIC-53, more Prxd4 exits the ER than ERp44 can capture. The less pronounced effects on Sumf1/FGE are not surprising, considering that this enzyme actively cycles along the early secretory pathway and—most importantly—is a client of ERGIC-53 (Fraldi et al., 2008). In the case of Sumf1, therefore, the paucity of ERp44 in distal compartment is compensated by its lower arrival in the absence of active ERGIC-53.

Figure 7 summarizes our view of how ERp44 and ERGIC-53 could synergize to couple transport efficiency and fidelity at the ER-Golgi interface. At the neutral pH of the ER, ERp44 and KDELR are in the OFF mode, while ERGIC-53 can bind its cargoes. ERGIC-53 and ERp44 interact with each other, likely in the vicinity of ERES, where secretory proteins that no longer interact with the ER matrix and passed the primary QC checkpoints preferentially arrive. Formation of these tripartite complexes may be important to stimulate the budding of vesicles that leave ERES via 4-PBA-sensitive mechanisms (Centonze and Farhan, 2019; Subramanian et al., 2019). In distal acidic compartments, ERGIC-53 releases its cargoes, which can be immediately inspected by nearby ERp44 molecules, ready to bind clients following pH- and zinc-dependent structural rearrangements (Vavassori et al., 2013; Watanabe et al., 2017, 2019). pH is probably more important than zinc in mediating the detachment of ERp44 from ERGIC-53. Zinc is not the only factor necessary for dissociation since endogenous and overexpressed ERp44 molecules are O-glycosylated and eventually secreted after prolonged TPEN treatments. pH, zinc, and clients themselves favor RDEL exposure (Sannino et al., 2014; Watanabe et al., 2019), facilitating the retrieval of client-ERp44 complexes by active KDELRs (Bräuer et al., 2019; Wilson et al., 1993; Wu et al., 2020). Also, ERGIC-53 returns to the ER, via COPI vesicles (Ben-Takaya et al., 2005).

Since the entry of zinc into the secretory compartment is mediated by antiporters exchanging the metal with protons, zinc concentration and pH are likely interdependent (Hara et al., 2017; Kambe et al., 2017; Kowada et al., 2020). Therefore, the synergic action of ERp44, ERGIC-53, and KDELR provides a pH- and zinc-regulated cycle that controls the localization and activity of a diverse set of clients, including ER-resident enzymes that can exert also important extracellular functions (Fraldi et al., 2008; Hisatsune et al., 2015; Zito et al., 2007). By coupling the transport of cargoes and QC inspector molecules, cells ensure efficiency and fidelity of protein secretion.

Limitations of the study

Our study describes a mechanism that may allow cells to increase the stringency of post-ER protein QC without jeopardizing transport efficiency. We show that the cycling lectin ERGIC-53 promotes the exit

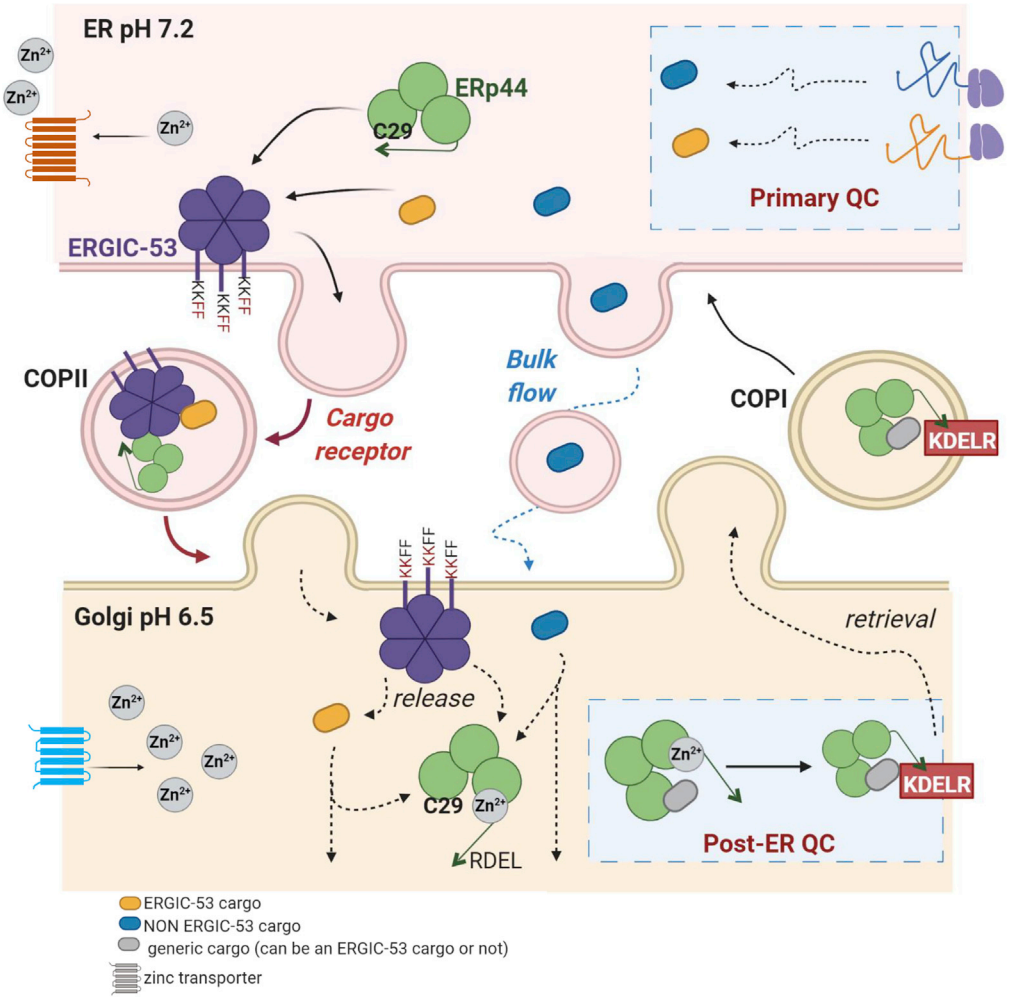

Figure 7. ERp44 and ERGIC-53 synergize to optimize post-ER quality control

Secretory proteins that pass the proximal quality control checkpoints exerted by ER-resident chaperones (BiP, PDI, CRT, etc.) arrive to ERES and can proceed toward the Golgi by bulk flow or with the help of cargo receptors that facilitate entry into COPII-coated vesicles (spHalo or spHalo-44ΔRDEL, respectively, in our experiments). In the neutral pH and low zinc environment of the ER, ERp44 and KDELR are in the OFF state, while ERGIC-53 captures its glycoprotein substrates though its luminal domain and interacts with Sec24 with its cytosolic FF motif. ERp44 binds to ERGIC-53 in the ER, promoting export toward the Golgi. Upon arrival in acidic and zinc-rich compartments, ERp44 detaches from ERGIC-53 and opens its tail, exposing the binding sites for clients and KDELR. ERGIC-53 releases its clients that can proceed toward the extracellular space or be captured by ERp44 and retrieved via KDELR. The simultaneous dissociation of the tripartite ERp44-ERGIC-53-client complex in a confined space may facilitate the binding of non-native clients by ERp44.

from the ER not only of its glycoprotein clients but also of the chaperone ERp44. Our findings do not exclude that ERp44 may interact with other cargo receptors. Similarly, ERGIC-53 could promote the cycling of other ER-resident chaperones and enzymes in post-ER compartments, as in the case of FGE/Sumf1. While we have confirmed the ERp44-ERGIC-53 liaison in several cell lines, we are aware that additional tissue-specific mechanisms be operative to favor the transport of select client proteins. Importantly, it remains to be understood how the two proteins interact and dissociate.

Resources availability

Lead contact

Further information and requests should be directed to and will be fulfilled by the lead contact, Tiziana Anelli (anelli.tiziana@hsr.it).

Materials availability

Materials (plasmids) generated in this study will be made available upon reasonable request to the lead contact. Their delivery could require a material transfer agreement.

Data and code availability

Not applicable.

METHODS

All methods can be found in the accompanying Transparent Methods supplemental file.

SUPPLEMENTAL INFORMATION

Supplemental information can be found online at https://doi.org/10.1016/j.isci.2021.102244.

ACKNOWLEDGMENTS

We thank Jeff Brodsky, Kenji Inaba, Maurizio Molinari, Iria Medrano-Fernandez, Jaakko Saraste, Eelco van Anken, and our lab members for helpful suggestions and discussions, the Advanced Light and Electron Microscopy BioImaging Center (ALEMBIC) of the I.R.C.C.S Ospedale San Raffaele, and, in particular, Valeria Berno for the technical support, and Samuel Zambrano for help with statistical analyses. This work is part of the PhD thesis of T.T. Roberto Sitia has received funding from AIRC under IG 2019 - ID. 23285 project, Telethon (GGP15059), and Ministero dell'Università e Ricerca (PRIN 2017XA5J5N).

AUTHOR CONTRIBUTIONS

Conceptualization, T.T., T.A., and R.S.; methodology, T.T., A.O., T.A., and E.D.Y.; investigation, T.T., A.O., D.S., T.A., and C.V.; writing – original draft, T.T., T.A., and R.S.; writing – review & editing, T.T., A.O., T.A., R.S., D.S., C.V., and E.D.Y.; fund acquisition, R.S.

DECLARATION OF INTERESTS

The authors declare no competing interests.

Received: December 11, 2020
Revised: February 1, 2021
Accepted: February 25, 2021
Published: March 19, 2021

REFERENCES

Anelli, T., Alessio, M., Bachi, A., Bergamelli, L., Bertoli, G., Camerini, S., Mezghrani, A., Ruffato, E., Simmen, T., and Sitia, R. (2003). Thiol-mediated protein retention in the endoplasmic reticulum: the role of ERp44. EMBO J. *22*, 5015–5022.

Anelli, T., Alessio, M., and Mezghrani, A. (2002). ERp44, a novel endoplasmic reticulum folding assistant of the thioredoxin family. EMBO J. *21*, 835–844.

Anelli, T., Ceppi, S., Bergamelli, L., Cortini, M., Masciarelli, S., Valetti, C., and Sitia, R. (2007). Sequential steps and checkpoints in the early exocytic compartment during secretory IgM biogenesis. EMBO J. *26*, 4177–4188.

Anelli, T., and Sitia, R. (2008). Protein quality control in the early secretory pathway. EMBO J. *27*, 315–327.

Appenzeller-Herzog, C., Roche, A.C., Nufer, O., and Hauri, H.P. (2004). pH-induced conversion of the transport lectin ERGIC-53 triggers glycoprotein release. J. Biol. Chem. *279*, 12943–12950.

Appenzeller, C., Andersson, H., Kappeler, F., and Hauri, H.P. (1999). The lectin ERGIC-53 is a cargo transport receptor for glycoproteins. Nat. Cell Biol. *1*, 330–334.

Barlowe, C., and Helenius, A. (2016). Cargo capture and bulk flow in the early secretory pathway. Annu. Rev. Cell Dev. Biol. *32*, 197–222.

Barlowe, C.K., and Miller, E.A. (2013). Secretory protein biogenesis and traffic in the early secretory pathway. Genetics *193*, 383–410.

Ben-Takaya, H., Miura, K., Pepperkok, R., and Hauri, H.P. (2005). Live imaging of bidirectional traffic from the ERGIC. J. Cell Sci. *118*, 357–367.

Borgese, N. (2016). Getting membrane proteins on and off the shuttle bus between the endoplasmic reticulum and the Golgi complex. J. Cell Sci. *129*, 1537–1545.

Borgese, N., Francolini, M., and Snapp, E. (2006). Endoplasmic reticulum architecture: structures in flux. Curr. Opin. Cell Biol. *18*, 358–364.

Bräuer, P., Parker, J.L., Gerondopoulos, A., Zimmermann, I., Seeger, M.A., Barr, F.A., and Newstead, S. (2019). Structural basis for pH-dependent retrieval of ER proteins from the Golgi by the KDEL receptor. Science *363*, 1103–1107.

Centonze, F.G., and Farhan, H. (2019). Crosstalk of endoplasmic reticulum exit sites and cellular signaling. FEBS Lett. *593*, 2280–2288.

Cortini, M., and Sitia, R. (2010). ERp44 and ERGIC-53 synergize in coupling efficiency and fidelity of IgM polymerization and secretion. Traffic *11*, 651–659.

Costantini, L., and Snapp, E. (2013). Probing endoplasmic reticulum dynamics using fluorescence imaging and photobleaching techniques. Curr. Protoc. Cell Biol. *60*, Unit 21.7.

D'Arcangelo, J.G., Stahmer, K.R., and Miller, E.A. (2013). Vesicle-mediated export from the ER:

COPII coat function and regulation. Biochim. Biophys. Acta *1833*, 2464–2472.

Fraldi, A., Zito, E., Annunziata, F., Lombardi, A., Cozzolino, M., Monti, M., Spampanato, C., Ballabio, A., Pucci, P., Sitia, R., and Cosma, M.P. (2008). Multistep, sequential control of the trafficking and function of the multiple sulfatase deficiency gene product, SUMF1 by PDI, ERGIC-53 and ERp44. Hum. Mol. Genet. *17*, 2610–2621.

Gilchrist, A., Au, C.E., Hiding, J., Bell, A.W., Fernandez-Rodriguez, J., Lesimple, S., Nagaya, H., Roy, L., Gosline, S.J.C., Hallett, M., et al. (2006). Quantitative proteomics analysis of the secretory pathway. Cell *127*, 1265–1281.

Hampe, L., Radjainia, M., Xu, C., Harris, P.W.R., Bashiri, G., Goldstone, D.C., Brimble, M.A., Wang, Y., and Mitra, A.K. (2015). Regulation and quality control of adiponectin assembly by endoplasmic reticulum chaperone ERp44. J. Biol. Chem. *290*, 18111–18123.

Hara, T., Takeda, T.aki, Takagishi, T., Fukue, K., Kambe, T., and Fukada, T. (2017). Physiological roles of zinc transporters: molecular and genetic importance in zinc homeostasis. J. Physiol. Sci. *67*, 283–301.

Hauri, H.P., Appenzeller, C., Kuhn, F., and Nufer, O. (2000). Lectins and traffic in the secretory pathway. FEBS Lett. *476*, 32–37.

Herzig, Y., Sharpe, H.J., Elbaz, Y., Munro, S., and Schuldiner, M. (2012). A systematic approach to pair secretory cargo receptors with their cargo suggests a mechanism for cargo selection by Erv14. PLoS Biol. *10*, e1001329.

Hisatsune, C., Ebisui, E., Usui, M., Ogawa, N., Suzuki, A., Mataga, N., Takahashi-Iwanaga, H., and Mikoshiba, K. (2015). ERp44 exerts redox-dependent control of blood pressure at the ER. Mol. Cell *58*, 1015–1027.

Kakihana, T., Araki, K., Vavassori, S., Iemura, S.I., Cortini, M., Fagioli, C., Natsume, T., Sitia, R., and Nagata, K. (2013). Dynamic regulation of Ero1α and peroxiredoxin 4 localization in the secretory pathway. J. Biol. Chem. *288*, 29586–29594.

Kambe, T., Matsunaga, M., and Takeda, T.A. (2017). Understanding the contribution of zinc transporters in the function of the early secretory pathway. Int. J. Mol. Sci. *18*, 1–18.

Kowada, T., Watanabe, T., Amagai, Y., Liu, R., Yamada, M., Takahashi, H., Matsui, T., Inaba, K., and Mizukami, S. (2020). Quantitative imaging of labile Zn(2+) in the Golgi apparatus using a localizable small-molecule fluorescent probe. Cell Chem. Biol. *27*, 1521–1531.e8.

Krikun, G., Mor, G., Alvero, A., Guller, S., Schatz, F., Sapi, E., Rahman, M., Caze, R., Qumsiyeh, M., and Lockwood, C.J. (2004). A novel immortalized human endometrial stromal cell line with normal progestational response. Endocrinology *145*, 2291–2296.

Kuehn, M.J., Herrmann, J.M., and Schekman, R. (1998). COPII-cargo interactions direct protein sorting into ER-derived transport vesicles. Nature *391*, 187–190.

Lai, C.W., Aronson, D.E., and Snapp, E.L. (2010). BiP availability distinguishes states of homeostasis and stress in the endoplasmic reticulum of living cells. Mol. Biol. Cell *21*, 1909–1921.

Ma, W., Goldberg, E., and Goldberg, J. (2017). ER retention is imposed by COPII protein sorting and attenuated by 4-phenylbutyrate. Elife *6*, 1–22.

Mariappan, M., Radhakrishnan, K., Dierks, T., Schmidt, B., and Von Figura, K. (2008). ERp44 mediates a thiol-independent retention of formylglycine-generating enzyme in the endoplasmic reticulum. J. Biol. Chem. *283*, 6375–6383.

Meier, S., Bohnacker, S., Klose, C.J., Lopez, A., Choe, C.A., Schmid, P.W.N., Bloemeke, N., Rührnößl, F., Haslbeck, M., Bieren, J.E.von, et al. (2019). The molecular basis of chaperone-mediated interleukin 23 assembly control. Nat. Commun. *10*, 1–12.

Meunier, L., Usherwood, Y.-K., Chung, K.T., and Hendershot, L.M. (2002). A subset of chaperones and folding enzymes form multiprotein complexes in endoplasmic reticulum to bind nascent proteins. Mol. Biol. Cell *13*, 4456–4469.

Miesenböck, G., De Angelis, D.A., and Rothman, J.E. (1998). Visualizing secretion and synaptic transmission with pH-sensitive green fluorescent proteins. Nature *394*, 192–195.

Mitrovic, S., Ben-Tekaya, H., Koegler, E., Gruenberg, J., and Hauri, H.-P. (2008). The cargo receptors Surf4, endoplasmic reticulum-Golgi intermediate compartment (ERGIC)-53, and p25 are required to maintain the architecture of ERGIC and Golgi. Mol. Biol. Cell *19*, 1976–1990.

Molinari, M., and Helenius, A. (1999). Glycoproteins form mixed disulphides with oxidoreductases during folding in living cells. Nature *402*, 90–93.

Mossuto, M.F., Sannino, S., Mazza, D., Fagioli, C., Vitale, M., Yoboue, E.D., Sitia, R., and Anelli, T. (2014). A dynamic study of protein secretion and aggregation in the secretory pathway. PLoS One *9*, e108496.

Munro, S., and Pelham, H.R. (1987). A C-terminal signal prevents secretion of luminal ER proteins. Cell *48*, 899–907.

Nufer, O., Kappeler, F., Guldbrandsen, S., and Hauri, H.P. (2003). ER export of ERGIC-53 is controlled by cooperation of targeting determinants in all three of its domains. J. Cell Sci. *116*, 4429–4440.

Otsu, M., Bertoli, G., Fagioli, C., Guerini-Rocco, E., Nerini-Molteni, S., Ruffato, E., and Sitia, R. (2006). Dynamic retention of Ero1alpha and Ero1beta in the endoplasmic reticulum by interactions with PDI and ERp44. Antioxid. Redox Signal. *8*, 274–282.

Qin, Y., Dittmer, P.J., Park, J.G., Jansen, K.B., and Palmer, A.E. (2011). Measuring steady-state and dynamic endoplasmic reticulum and Golgi Zn2+ with genetically encoded sensors. Proc. Natl. Acad. Sci. U S A *108*, 7351–7356.

Raote, I., Ortega-Bellido, M., Santos, A.J., Foresti, O., Zhang, C., Garcia-Parajo, M.F., Campelo, F., and Malhotra, V. (2018). TANGO1 builds a machine for collagen export by recruiting and spatially organizing COPII, tethers and membranes. Elife *7*, e32723.

Reddy, P., Sparvoli, A., Fagioli, C., Fassina, G., and Sitia, R. (1996). Formation of reversible disulfide bonds with the protein matrix of the endoplasmic reticulum correlates with the retention of unassembled Ig light chains. EMBO J. *15*, 2077–2085.

Rubenstein, R.C., and Zeitlin, P.L. (1998). A pilot clinical trial of oral sodium 4-phenylbutyrate (Buphenyl) in deltaF508-homozygous cystic fibrosis patients: partial restoration of nasal epithelial CFTR function. Am. J. Respir. Crit. Care Med. *157*, 484–490.

Sannino, S., Anelli, T., Cortini, M., Masui, S., Degano, M., Fagioli, C., Inaba, K., and Sitia, R. (2014). Progressive quality control of secretory proteins in the early secretory compartment by ERp44. J. Cell Sci. *127*, 4260–4269.

Shibuya, A., Margulis, N., Christiano, R., Walther, T.C., and Barlowe, C. (2015). The Erv41-Erv46 complex serves as a retrograde receptor to retrieve escaped ER proteins. J. Cell Biol. *208*, 197–209.

Snapp, E.L., Sharma, A., Lippincott-Schwartz, J., and Hegde, R.S. (2006). Monitoring chaperone engagement of substrates in the endoplasmic reticulum of live cells. Proc. Natl. Acad. Sci. U S A *103*, 6536–6541.

Subramanian, A., Capalbo, A., Iyengar, N.R., Rizzo, R., di Campli, A., Di Martino, R., Lo Monte, M., Beccari, A.R., Yerudkar, A., del Vecchio, C., et al. (2019). Auto-regulation of secretory flux by sensing and responding to the folded cargo protein load in the endoplasmic reticulum. Cell *176*, 1461–1476.e23.

Sun, Z., and Brodsky, J.L. (2019). Protein quality control in the secretory pathway. J. Cell Biol. *218*, 3171–3187.

Tempio, T., and Anelli, T. (2020). The pivotal role of ERp44 in patrolling protein secretion. J. Cell Sci. *133*, jcs240366.

Thor, F., Gautschi, M., Geiger, R., and Helenius, A. (2009). Bulk flow revisited: transport of a soluble protein in the secretory pathway. Traffic *10*, 1819–1830.

Vavassori, S., Cortini, M., Masui, S., Sannino, S., Anelli, T., Caserta, I.R., Fagioli, C., Mossuto, M.F., Fornili, A., vanAnken, E., et al. (2013). A pH-regulated quality control cycle for surveillance of secretory protein assembly. Mol. Cell *50*, 783–792.

Watanabe, S., Amagai, Y., Sannino, S., Tempio, T., Anelli, T., Harayama, M., Masui, S., Sorrentino, I., Yamada, M., Sitia, R., and Inaba, K. (2019). Zinc regulates ERp44-dependent protein quality control in the early secretory pathway. Nat. Commun. *10*, 603.

Watanabe, S., Harayama, M., Kanemura, S., Sitia, R., and Inaba, K. (2017). Structural basis of pH-dependent client binding by ERp44, a key regulator of protein secretion at the ER-Golgi interface. Proc. Natl. Acad. Sci. U S A *114*, E3224–E3232.

Wendeler, M.W., Paccaud, J.P., and Hauri, H.P. (2007). Role of Sec24 isoforms in selective export of membrane proteins from the endoplasmic reticulum. EMBO Rep. *8*, 258–264.

Wilson, D.W., Lewis, M.J., and Pelham, H.R. (1993). pH-dependent binding of KDEL to its receptor in vitro. J. Biol. Chem. *268*, 7465–7468.

Wu, Z., Newstead, S., and Biggin, P.C. (2020). The KDEL trafficking receptor exploits pH to tune the strength of an unusual short hydrogen bond. Sci. Rep. *10*, 1–12.

Yang, K., Li, D.F., Wang, X., Liang, J., Sitia, R., Wang, C.chen, and Wang, X. (2016). Crystal structure of the ERp44-peroxiredoxin 4 complex reveals the molecular mechanisms of thiol-mediated protein retention. Structure *24*, 1755–1765.

Zeyen, L., Döring, T., and Prange, R. (2020). Hepatitis B virus exploits ERGIC-53 in conjunction with COPII to exit cells. Cells *9*, 1889.

Zhang, Y.C., Zhou, Y., Yang, C.Z., and Xiong, D.S. (2009). A review of ERGIC-53: its structure, functions, regulation and relations with diseases. Histol. Histopathol. *24*, 1193–1204.

Zito, E., Buono, M., Pepe, S., Settembre, C., Annunziata, I., Surace, E.M., Dierks, T., Monti, M., Cozzolino, M., Pucci, P., et al. (2007). Sulfatase modifying factor 1 trafficking through the cells: from endoplasmic reticulum to the endoplasmic reticulum. EMBO J. *26*, 2443–2453.

iScience, Volume *24*

Supplemental information

A virtuous cycle operated by ERp44 and ERGIC-53 guarantees proteostasis in the early secretory compartment

Tiziana Tempio, Andrea Orsi, Daria Sicari, Caterina Valetti, Edgar Djaha Yoboue, Tiziana Anelli, and Roberto Sitia

SUPPLEMENTAL ITEMS

Supplementary figures

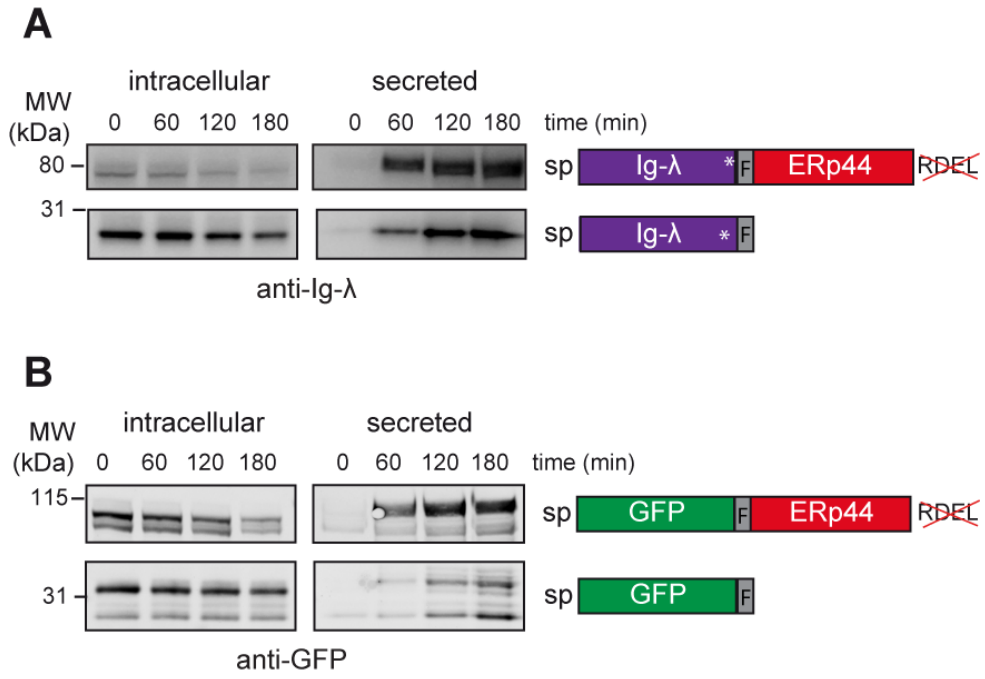

Figure S1. Appending ERp44ΔRDEL increases the velocity of secretion of different proteins (related to Fig.1A). HeLa cells transiently expressing Igλ-44ΔRDEL and Igλ (**A**) or spGFP and spGFP-44ΔRDEL (**B**) were cultured in the presence of puromycin and proteasome inhibitor MG132 for the indicated time, and then lysates (intracellular) and supernatants (secreted) were collected and resolved by reducing SDS-PAGE. Aliquots corresponding to $2x10^5$ cells for the intracellular or 10^6 cells for the secreted fraction were loaded per lane. Blots were decorated with anti-Igλ or anti-GFP respectively. Both ERp44 containing chimeras are secreted faster than their counterpart without ERp44, as shown by faster appearance in the secreted material and disappearance from the intracellular pool. The multiple forms observed for GFP chimeras are due to the presence of a N-glycosylation site at Asn28 – just between the SP and GFP itself, that is later processed in the Golgi. All proteins carries a signal peptide (SP) for ER targeting and a FLAG-tag, after Igλ and GFP respectively. ERp44 lacks its C-terminal RDEL retrieval motif while the C-Terminal cysteine of Igλ was removed to avoid thiol mediated retention and facilitate secretion (schematic of chimera used in right panel A and B).

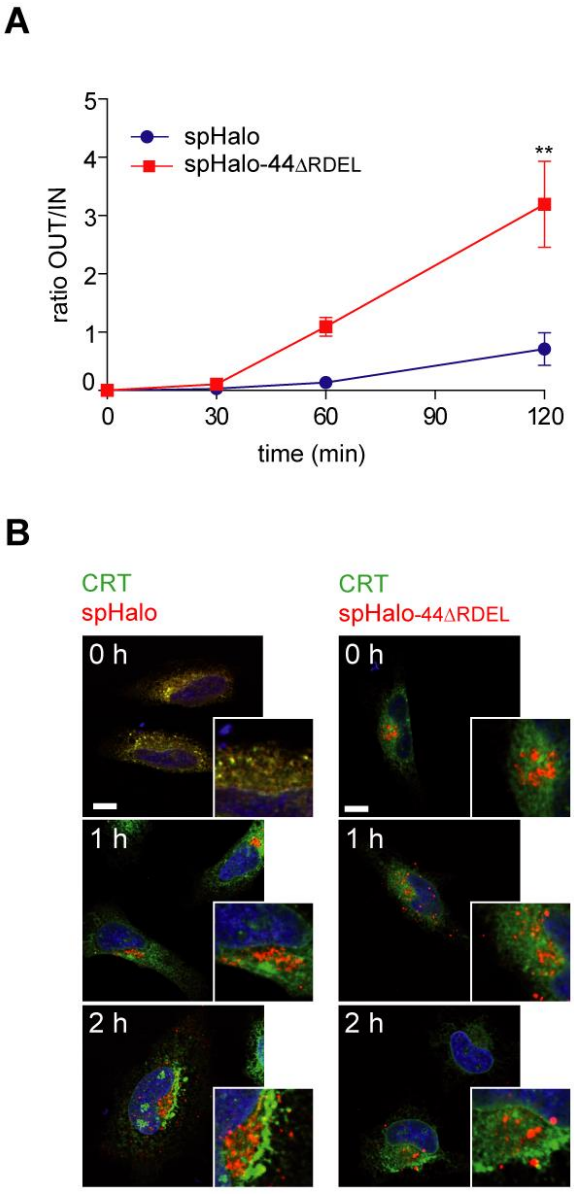

Figure S2. spHalo-44ΔRDEL travels faster along the secretory pathway than spHalo (related to Fig.1 A and E).
A) spHalo-44ΔRDEL and spHalo HeLa transfectants were pulse labelled with ^{35}S-labeled methionine and cysteine for 10 min and chased for the indicated times with excess cold amino acids. Cell lysates and supernatants were then incubated with immobilized Halo-ligand beads and, after careful washing, the radioactivity present on beads was measured in a scintillation counter. spHalo-44ΔRDEL was secreted more efficiently than spHalo. Secretion of Halo-tagged proteins (spHalo and spHalo-44ΔRDEL) is expressed as the percentage of radioactive signal in the secreted medium relative to the intracellular signal at the beginning of chase (Average of 2 independent experiments +/- SEM). **B)** Visual pulse-chase. Cells were treated as in figure 1E. The colocalization between spHalo or spHalo-44ΔRDEL (red) and ER marker Calreticulin (CRT, green) is shown. At the beginning of chase (20 min after synthesis) spHalo shows strong colocalization with CRT while spHalo-44ΔRDEL has already left the compartment.
Scale bar = 10 µm, valid for all images. Zoom panels show regions of interest magnified 2.9 fold. 20 cells for each transfectant and each time point were analyzed in 3 independent experiments; representative images are shown in the panels.

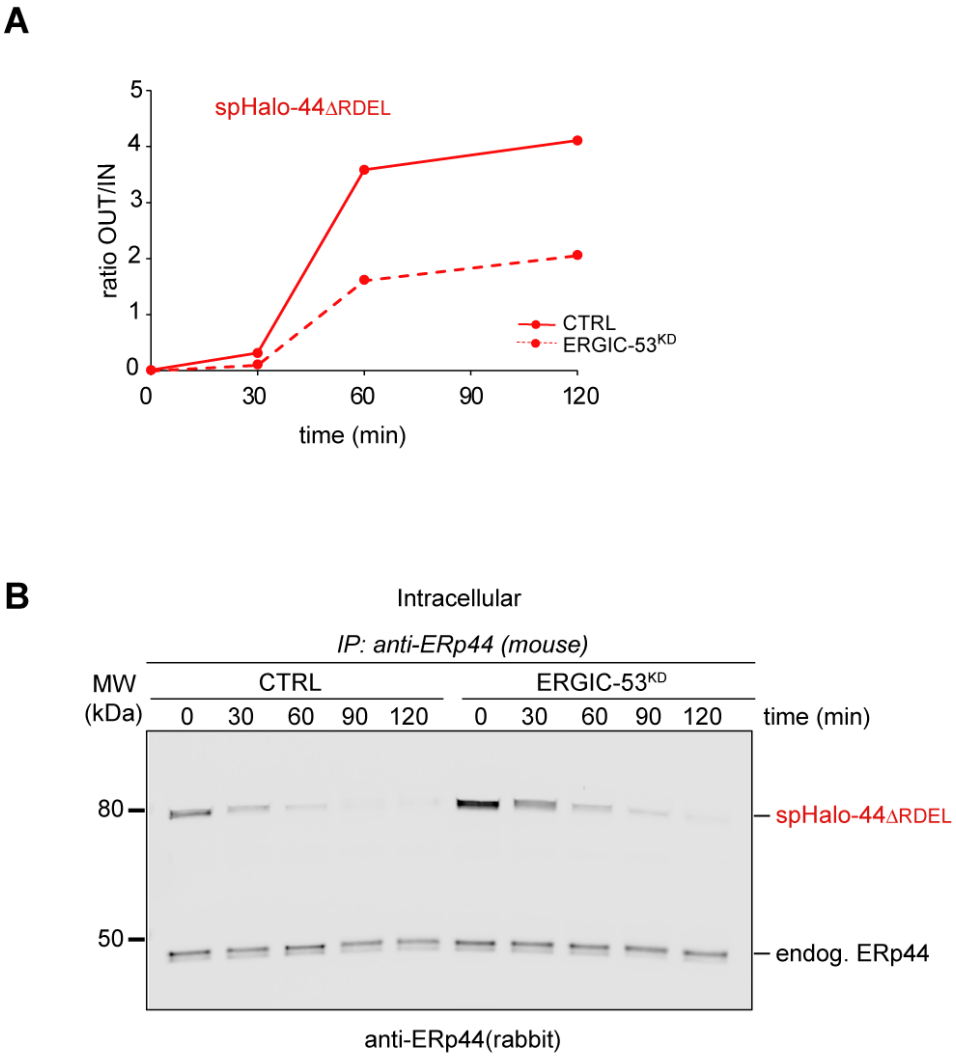

Figure S3. ERGIC-53 levels control spHalo-44ΔRDEL secretion (related to Fig.3).
A) HeLa transfectants expressing spHalo-44ΔRDEL were treated with ERGIC-53 (ERGIC-53^{KD}) or control (CTRL) duplexes and pulse labelled with ^{35}S-labeled methionine and cysteine as described in Figure S1. Samples were precipitated with anti-ERp44 antibodies resolved by SDS-PAGE and the bands of interest quantified by densitometry. The graph confirms that the presence of ERGIC-53 allows faster secretion of spHalo-44ΔRDEL.
B) Lysates from a radioactive pulse chase of HeLa cells treated with ERGIC-53 (ERGIC-53^{KD}) or control (CTRL) duplexes were precipitated with anti-ERp44 antibodies. The chase was performed in the presence of puromycin. The IP material was analyzed by reducing SDS-PAGE, followed by immunoblotting for ERp44. While the signal of endogenous ERp44 remains constant, there is an intracellular accumulation of the chimera spHalo-44ΔRDEL in the absence of ERGIC-53.

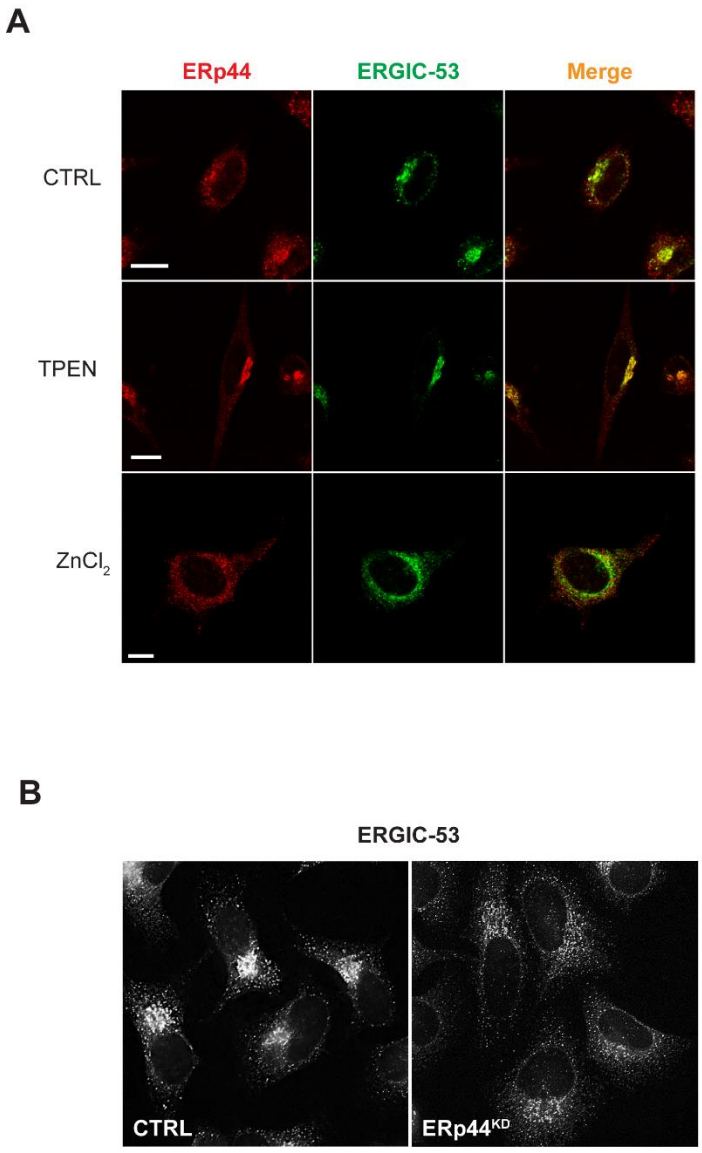

Figure S4. Zinc modulation affects ERp44 and ERGIC-53 localization in HeLa cells (related to Fig.6).
A) The subcellular localization of endogenous ERp44 and ERGIC-53 was analyzed in HeLa cells upon zinc deprivation (10 µM TPEN for 30min) or enrichment (20 µM $ZnCl_2$ for 3 hours). ERp44 and ERGIC-53 partially co-localize at steady state (upper panels). Both ERp44 and ERGIC-53 accumulate in the Golgi area in the absence of zinc (middle panels), while zinc addition yields a reticular distribution that likely corresponds to the ER (bottom panels). Scale bar = 10 µm. The same phenotype was observed in more than 20 cells for each condition in three independent experiments.
B) ERGIC-53 adopts a reticular staining pattern upon ERp44 silencing. Scale bar = 10 µm. The same phenotype was observed in more than 25 cells for each condition in two independent experiments.

Transparent Methods

Cells, plasmids, vectors, transfection and RNAi

HeLa cells S3 were obtained from ATCC and were cultured in DMEM (Gibco, Invitrogen) supplemented with 10% Fetal Bovine Serum (Euroclone), Pen/Strep. T-HESC cells, originated from normal human endometrial stromal cell immortalized with hTERT (Krikun et al., 2004), were obtained from ATCC (CRL-4003™). Cells were maintained in complete growth medium supplemented with 10% charcoal treated FBS (Sigma St Louis, MO) according to the manufacturer's instructions.

spHalo was built by amplifying the plasmid Halo-ERp44 pcDNA3.1 (-) (Mossuto et al., 2014) with the following primers (FW: ACGACTCACTATAGGGAGAC; RV:GGGGGTACCTTTAGGATCCGCCGGAAATCTCGAGCGTC).

The PCR product (containing a stop codon after Halo coding sequence) was subsequently cloned into the pcDNA 3.1 (-) vector using XbaI and KpnI restriction sites and validated by sequencing.

spHalo-44ΔRDEL in pcDNA3.1(-) was generated by swapping the 1007 Kb HindIII fragment from plasmid HA-ERp44ΔRDEL pcDNA3.1(-) (Anelli et al., 2003) with the corresponding HindIII fragment from Halo-ERp44 pcDNA3.1(-) (Mossuto et al., 2014). Prdx4-FLAG in pcDNA3.1- was previously described (Kakihana et al., 2013). Vectors encoding Myc-tagged, glycosylated human wild-type ERGIC-53 (GM-ERGIC-53) (Appenzeller et al., 1999) was a kind gift from Hans-Peter Hauri (Biozentrum, University of Basel, Switzerland).

The construct for the expression of a secretable Ig lambda chain (spIgλ) was generated by PCR amplification of murine immunoglobulin light chain lambda (Reddy et al., 1996) with the following primers: FW-CGGGATCCATTATGGCCTGGATTTCACTT; RV- TTG GGC CCT CAT CTA GAC TTG TCA TCG TCA TCC TTG TAG TCA GCA CGG GAC AAA CTC TTCTC.

These introduce a C-terminal FLAG tag and remove the C-terminal cysteine of lambda. The fragment was then inserted into pCDNA 3.1+ vector using BamHI and ApaI sites.

Similarly, spGFP chimera was generated introducing a C-Terminal FLAG tag by PCR amplification of mEGFP with the following primers: FW-CGGGATCCACCATGGCACCCCTGAGACCC; RV-TTG GGC CCT CAT CTA GAC TTG TCA TCG TCA TCC TTG TAG TCC TTG TAC AGC TCG TCC ATG CCG AG. The fragment was then inserted into pCDNA 3.1+ vector using BamHI and ApaI sites.

The construct for the expression of Igλ-ERp44ΔRDEL and GFP-ERp44ΔRDEL chimeras were instead obtained by PCR amplification of spHalo-ERp44 plasmid, with primers: FW:–CCGGGCTAGCGAAATAACAAGTCTTGATAC; RV: CGATGGGCCCTAATCCCTCAATAGAGTATACC. PCR products were then digested with ApaI and NheI and cloned using XbaI and ApaI sites into spIgλ and spGFP plasmids, to generate respectively spIgλ-ERp44ΔRDEL and spGFP-ERp44ΔRDEL expression constructs. All plasmids were confirmed by sequencing.

Cells were transfected with JET PEI reagent (Euroclone) ≥48 hours before analysis following the manufacturer's instructions. siRNA specific (Sigma-Aldrich) for ERp44 and ERGIC-53 have been previously described (Anelli et al., 2002, 2007).
Cells were silenced using Lipofectamine RNAiMAX (Invitrogen) following the manufacturer's instructions and analyzed after 72 hours. When cells were both silenced and transfected, silencing was performed 24 h prior to transfection and cells assayed after 72 hours from silencing.

Secretion assays

Secretion assays were performed in Opti-MEM (Gibco, Invitrogen), using 10^6 cells per time point. Hela cells transiently transfected with spHalo and spHalo-44ΔRDEL were detached using trypsin-EDTA, washed in PBS and resuspended in Opti-MEM (Invitrogen) at the concentration of 10^6 cells/mL.
Supernatants were collected and cleared at 13,000 rpm for 1 min, while cell pellets were washed in PBS containing 10 mM NEM (Sigma-Aldrich), to block disulphide exchange, and then lysed in RIPA buffer (150 mM NaCl, 50 mM Tris-HCl pH 7.5, 1% NP40, 0.5% Na Deoxycholate, 0.1% SDS) supplemented with complete protease inhibitors (Roche) and 10 mM NEM. Lysates and supernatants corresponding to $2x10^5$ cells were analyzed by western blotting using rabbit polyclonal anti-Halo antibodies (Promega) 1:1000 over night in PBS 0.1% Tween 20.
Secretion for GFP and Igλ chimeras, were performed in Optimem supplemented with 2 μg/mL Puromycin and 10 μM MG132 to block de novo protein synthesis and proteasome degradation. Blots were then decorated respectively with: rabbit anti-GFP antibody, Alexa

647 conjugated (Invitrogen #A31852) 1:1000; or goat anti mouse Lambda-HRP (Southern Biotech, #1060-05) 1:1000.

Secretion assay for Prdx4 analysis was performed in Opti-MEM (Gibco, Invitrogen), using 10^6 cells per time point. Secreted materials were precipitated with 15% trichloroacetic acid (TCA) and then resolved by SDS-PAGE under reducing conditions. Lysates and supernatants were analyzed by western blotting using rabbit polyclonal anti-Prdx4 (Proteintech, 1:1000) over night in PBS 0.1% Tween 20.

Non-radioactive Halo-ligand pulse chase

HeLa cells silenced with ERGIC-53-specific or irrelevant duplexes (Anelli et al., 2007), were transfected with spHalo or spHalo-44ΔRDEL plasmids. Equal amounts of cells were incubated for 2 hours at 37°C in complete medium supplemented with 30 µM 6-Chlorohexanol (Sigma) (a colorless Halo ligand), washed in PBS and incubated for 20 min at 37°C with 100 nM TMR Direct Halo ligand (pulse). After two washes in ice cold PBS containing 30 µM 6-Chloroexanol and 2 µg/mL puromycin (Sigma), cells were incubated for the desired chase times at 37°C in Opti-MEM supplemented with 30µM 6-Chlorohexanol and puromycin. $1.5x10^6$ cells were used per time point for secretion assays. Supernatants and lysates corresponding to $2x10^5$ cells were loaded on 4-12% precast gel (Invitrogen) and Fluorescent TMR Direct Halo ligand signal was detected directly on gel by Typhoon FLA 9000 scanner (GE) and analyzed using ImageJ software. The same protocol was used also in the presence of 4-phenylbutyrate (4-PBA) (Sigma). In this case, HeLa cells were incubated with 10mM 4-PBA in the first 2 hours in presence of 30µM 6-Chlorohexanol, during the pulse and also during the chase.

Immunoprecipitation and Western blotting

For enrichment of spHalo and spHalo-ERp44WT HeLa transfectants were washed with PBS 10 mM NEM and lysed in 100 mM NaCl, 50 mM Hepes pH 7.5, 1% NP40. Lysate aliquots corresponding to 1 mg protein were pre-cleared for 1 hour at 4°C with Sepharose beads cross-linked to FCS proteins upon CNBr activation (home-made) to reduce unspecific binding, and then incubated over night with 10 µL of Halo-link resin (Promega). All buffers were supplemented with 2 mM $Ca^{2+}$and Mg^{2+} to preserve ERGIC-53 activity. Aliquots before and after enrichment were analyzed to verify transgene expression and precipitation efficiency.

For co-immunoprecipitation of ERp44 (mock, HA or Halo tagged) and ERGIC-53 (mock and Glyco-myc tagged GM-ERGIC-53) (Appenzeller et al., 1999), HeLa transfectants were treated as described above. Lysate aliquots corresponding to 500 µg of total proteins were precleared for 1 h at 4°C with FCS-Sepharose beads and incubated over night with 10 µL of mouse monoclonal ERp44 antibody (36C9, in-house) (Anelli et al., 2007) DMP (dimethyl pimelimidate) cross-linked to protein G-Agarose (PGA) beads (Promega).

Co-immunoprecipitated material was eluted from the beads in reducing Laemmli buffer and resolved on 4-12% precast poly-acrylamide gels (ThermoFischer). After transfer onto nitrocellulose, blots were decorated with polyclonal anti-ERGIC-53 (Sigma Aldrich, 1:500), anti-Halo (Promega 1:1000) or anti-ERp44 rabbit polyclonal (Proteintech, 1:500) followed by Alexa-conjugated secondary antibodies (Invitrogen 1:1000). Fluorescent signals were acquired on a Typhoon FLA 9000 scanner (GE).

Radioactive pulse chases

Cells silenced and/or transfected as above, were resuspended at 10^7 cell/mL in DMEM without methionine and cysteine (Invitrogen) supplemented with 1% dialyzed FBS. After 20 min at 37°C, cells were pulsed for 10 min with 33 µCi/10^6 cells of ^{35}S-labeled methionine and cysteine (EasyTag, Perkin Elmer), washed twice in PBS and chased in Opti-MEM with 2.5 mM cold Methionine, for the desired chase times. For analysis of total radioactivity, supernatants and cell lysates were precipitated with Halo-link beads as described above. Beads were subjected to different washing steps to get rid of associated proteins: firstly with solution 'a' (500 mM NaCl, 10 mM Tris-HCl pH 7.5, 0.5% NP40, 0.05% SDS), then in STN (150 mM NaCl, 10 mM Tris-HCl pH7, 0.025% NP-40) supplemented with 100 mM DTT and once more in STN buffer supplemented with 100 mM NEM. Total radioactivity associated with spHalo or spHalo-44ΔRDEL was quantified in a beta scintillation counter (Perkin Elmer), adding beads to 5 mL of UltimaGold scintillation solution. For radioactive secretion of ERp44, cell lysates were precipitated with 10 µl of mouse anti-ERp44 (36C9, in-house, 1:1000); for radioactive secretion of Prdx4-FLAG, lysates were precipitated O/N at 4°C with 10 µl of anti-FLAG beads (Sigma, cat#A2220). Beads were washed with solution 'a', then with STN buffer and finally with 10 mM Tris-HCl pH 7.4. Immunoprecipitated material was eluted from the beads in reducing Laemmli buffer, and resolved by 4-12%, 1-mm precast poly-acrylamide gels (ThermoFischer). Gel was dried on 3MM paper under vacuum for 90 min at 80°C and then

exposed to LE storage phosphor screen (Amhersham). Radioactive signal acquired on a Typhoon FLA 9000 scanner (GE).

Immunofluorescence analysis

HeLa transfectants expressing spHalo or spHalo-44ΔRDEL were incubated for 2 hours with TMR-Direct Halo ligand (Promega, 100nM) then fixed in 4% PFA, permeabilized in PBS/0.1% TritonX-100, blocked with PBS/ 10% FCS for 1h at room temperature and labelled with rabbit anti-CRT (Sigma Cat#C4606, 1:250) and mouse anti-GM130 (BectonDickinson Cat#710823, 1:500) antibodies in combination. For the visual Halo-pulse chase experiment, all Halo molecules (spHalo-44ΔRDEL or spHalo) are saturated with 30μM of 6-Chlorohexanol (Sigma), an unlabeled Halo-ligand. Then newly synthesized Halo molecules were labeled with a fluorescent TMR-Direct Halo ligand (Promega, 100nM) for 20 min (pulse). Cells were then cultured in the presence of unlabeled ligands and puromycin, to block the synthesis of new proteins, fixed and analyzed by fluorescence microscopy at the indicated times (0, 1 hour, 2 hour) (chase). Fluorescent images were obtained using a confocal microscope (Leica SP8) equipped with a 40x oil-immersion objective lens in the ALEMBIC Facility of Ospedale San Raffaele.

To analyze the localization of endogenous ERp44 and ERGIC-53 in both T-HESC and HeLa, cells plated onto glass coverslips were incubated in Opti-MEM containing 10μM TPEN **(**N,N,N′,N′-Tetrakis(2-pyridylmethyl)ethylenediamine) for 30 min or 20 μM $ZnCl_2$ for 3 h. Cells were fixed in 4% PFA, permeabilized in PBS/0.1% TritonX-100 and blocked with PBS/ 10% FCS for 1h at room temperature. Cells were then incubated with antibodies against ERp44 (rabbit JDA1 purified, in-house, 1:250) (Ronzoni et al., 2010), ERGIC-53 (G1/93) (Schweizer et al., 1988) and GM130 (rabbit 1:1000, kindly provided by A. De Matteis, TIGEM, Naples) for 30 min, followed by Alexa-conjugated secondary antibodies (Invitrogen 1:500). Fluorescent images were obtained using a confocal microscope (Leica SP2) equipped with a 40x oil-immersion objective lens or using a GE Healthcare DeltaVision™ Ultra microscope and 60x objective lens for Fig S4B.

Pearson's correlation coefficient values were calculated using the Volocity software (PerkinElmer).

Supplemental References

Ronzoni, R., Anelli, T., Brunati, M., Cortini, M., Fagioli, C., & Sitia, R. (2010). Pathogenesis of ER storage disorders: modulating Russell body biogenesis by altering proximal and distal quality control. *Traffic (Copenhagen, Denmark)*, *11*(7), 947–957.

Schweizer, A., Fransen, J. A., Bächi, T., Ginsel, L., & Hauri, H. P. (1988). Identification, by a monoclonal antibody, of a 53-kD protein associated with a tubulo-vesicular compartment at the cis-side of the Golgi apparatus. *The Journal of Cell Biology*, *107*(5), 1643–1653.